

Copyright
by
Jennifer Yuxin Wang
2020

**The Dissertation Committee for Jennifer Yuxin Wang Certifies that this is the
approved version of the following dissertation:**

***Ehrlichia chaffeensis* E3 Ligase TRP120 Ubiquitinates Tumor
Suppressor FBW7 for Degradation to Promote Infection**

Committee:

Jere W. McBride, Ph.D., Mentor, Chair

Ashok K. Chopra, Ph.D.

Joao H. F. Pedra, Ph.D.

Shao-Jun Tang, Ph.D.

David H. Walker, M.D.

***Ehrlichia chaffeensis* E3 Ligase TRP120 Ubiquitinates Tumor
Suppressor FBW7 for Degradation to Promote Infection**

by

Jennifer Y. Wang, B.S.

Dissertation

Presented to the Faculty of the Graduate School of
The University of Texas Medical Branch
in Partial Fulfillment
of the Requirements
for the Degree of

Doctor of Philosophy

**The University of Texas Medical Branch
May, 2020**

Dedication

To my parents and my three furbabies

Acknowledgements

There are so many people I'd like to thank for helping me getting through this particular journey of my life. Ph.D. is a challenging one and without their support, it would not have been possible.

I would like to express my deepest appreciation to my mentor, Dr. Jere McBride. His guidance and support were the GPS to my long journey here at UTMB. Without them, I would have been groping through the dark and probably fallen into a ditch or walked into a lake a couple of times. His patience and advice taught me what it takes to be the scientist I am today and the lessons from him will continue to shape me throughout the rest of my career. I am also extremely grateful to my dissertation committee members, Drs. Ashok Chopra, Joao Pedra, Shao-Jun Tang and David Walker, for their time, advice and expertise that shaped this project over the years.

Many sincere thanks to my past and present lab mates. Xiaofeng Zhang was the lab mom everyone needed, she was always available to give support and advice. Bing Zhu for many helpful discussions and all the suggestions that helped making this project better. Tierra Farris for showing me the ropes when I first joined and offered so much support in and outside the lab. Tian Luo and Sudha Velayutham for always being patient with helping me with protocols and answering my questions. My lab experience would not be the same if not for those interesting philosophical discussions about life with

Shubhajit Mitra. Towards the second half of my Ph.D., Madison Rogan became one of the best lab partners one could ask for, especially during late and weekend work hours. Without her, the Swear Jar would not have been possible. LaNisha Patterson for her tenacious and positive attitude towards work and life, and for those infectious (pun unintended) laughs that can brighten even the worst days. Caitlan Byerly for reminding me being optimistic was the best way to start and end a day. Of course, I couldn't leave here without thanking Jignesh Patel for his support and tolerance of my quirks. All in all, with them many laughs and tears were shared, and work got done!

It was a long and winding path to finally reach the destination of this journey. I am eternally indebted to my family and friends for keeping this road so well lit. Their love and continual support kept me grounded and reminded me to be kind to myself when things got rough.

(Just a bit of thanks to COVID-19 for keeping me inside to finish this writing)

***Ehrlichia chaffeensis* E3 Ligase TRP120 Ubiquitinates Tumor Suppressor FBW7 for Degradation to Promote Infection**

Publication No. _____

Jennifer Y. Wang, Ph.D.

The University of Texas Medical Branch, 2020

Supervisor: Jere W. McBride

Ehrlichia chaffeensis (*E. chaffeensis*) exploits evolutionarily conserved Notch and Wnt host cell signaling pathways to downregulate innate immune host defenses and promote infection. The multifunctional *E. chaffeensis* TRP120 effector which has HECT E3 ubiquitin ligase activity, interacts with the host nuclear tumor suppressor F-BOX and WD domain repeating-containing 7 (FBW7). FBW7 is the substrate recognition subunit of the Skp1-cullin-1-FBOX E3 ubiquitin (Ub) ligase complex (SCF) known to negatively regulate a network of oncoproteins (Notch, cyclin E, c-Jun, MCL1 and cMYC). In this study, we demonstrate that TRP120 and FBW7 colocalize strongly in the nucleus by confocal immunofluorescent microscopy and interactions between TRP120 and FBW7 FBOX and WD40 domains were demonstrated by ectopic expression and co-immunoprecipitation. Although *FBW7* gene expression increased during *E. chaffeensis* infection, FBW7 levels significantly decreased (>70%) by 72 h post infection. Moreover, an iRNA knockdown of FBW7 coincided with increased *E. chaffeensis* infection and levels of Notch intracellular domain (NICD), phosphorylated c-Jun, MCL-1 and cMYC,

which are negatively regulated by FBW7. An increase in FBW7 K48 ubiquitination was detected during infection by co-IP, and FBW7 degradation was inhibited in infected cells treated with the proteasomal inhibitor bortezomib. Direct TRP120 ubiquitination of native and recombinant FBW7 was demonstrated *in vitro* and confirmed by ectopic expression of TRP120 HECT Ub ligase catalytic site mutant. This study identifies the tumor suppressor, FBW7, as a TRP120 HECT E3 Ub ligase substrate, and demonstrates that TRP120 ligase activity promotes ehrlichial infection by degrading FBW7 to maintain stability of Notch and other oncoproteins involved in cell survival and apoptosis.

TABLE OF CONTENTS

List of Figures	ix
List of Abbreviations	x
Chapter 1. Introduction	12
<i>Ehrlichia chaffeensis</i> and Human Monocytotropic Ehrlichiosis	12
<i>Ehrlichia chaffeensis</i> Lifecycle	14
Tandem Repeat Proteins and Other Bacterial Moonlight Effectors	16
Overview of Bacterial Nucleomodulins and Interaction with The Host Cells	20
Bacterial Ubiquitin Ligases	23
Tumor Suppressor FBW7	24
Project Introduction	27
Chapter 2. Materials and Methods	29
Chapter 3. <i>Ehrlichia chaffeensis</i> TRP120-Mediated Ubiquitination and Proteasomal Degradation of Tumor Suppressor FBW7 Increases Oncoprotein Stability and Promotes Infection	35
Introduction.....	35
Results.....	38
<i>E. chaffeensis</i> TRP120 interacts with human SCF ligase FBW7.	38
TRP120 interacts with the FBOX and WD40 domains of FBW7.	40
FBW7 is degraded during <i>E. chaffeensis</i> infection.....	42
FBW7 degradation results in increased levels of FBW7 regulated oncoproteins.....	45
FBW7 degradation during infection is K48-Ub-dependent.....	47
TRP120 ubiquitinates FBW7 for degradation.	49
Changes in FBW7 levels impact <i>E. chaffeensis</i> infection.	51
Discussion.....	52
Chapter 4. Summary and Future Directions	60
References	63
Curriculum Vitae	79

List of Figures

Figure 1:	<i>E. chaffeensis</i> TRP120-FBW7 nuclear colocalization and interaction with FBW7 FBOX and WD40 domains.....	39
Figure 2:	Direct interaction between TRP120-TR with FBW7 domains.....	41
Figure 3:	FBW7 is degraded during <i>E. chaffeensis</i> infection.....	44
Figure 4:	Levels of FBW7-regulated oncoproteins are increased during <i>E. chaffeensis</i> infection.....	46
Figure 5:	FBW7 is ubiquitinated with K48-Ub and degraded by the proteasome.....	48
Figure 6:	<i>E. chaffeensis</i> TRP120 HECT E3 Ub ligase activity mediates K48 ubiquitination and degradation of FBW7.	49
Figure 7:	Changes in FBW7 levels impact <i>E. chaffeensis</i> infection.	51
Figure 8:	Proposed model of <i>E. chaffeensis</i> TRP120 HECT E3 ligase regulation of FBW7 during infection.	58

List of Abbreviations

Ctrl	Control
DAPI	4',6-diamidino-2-phenylindole
DC	Dense-cored cell
DNA	Deoxyribonucleic acid
FBS	Fetal bovine serum
FBW7	F-Box and WD domain repeat-containing 7
HeLa	Henrietta Lack's cervical epithelial adenocarcinoma cells
HECT	Homologous to the E6-AP carboxyl terminus
hpi	Hours post-infection
IP	Immunoprecipitation
KD	Knockdown
kDa	Kilodalton
LAMP2	Lysosome-associated membrane protein 2
LC3	Microtubule-associated protein 1A/1B-light chain 3
LPS	Lipopolysaccharide
MCL1	Induced myeloid leukemia cell differentiation protein
MOI	Multiplicity of infection
NEM	<i>N</i> -ethylmaleimide
NICD	Notch intracellular domain
PCGF5	Polycomb group ring finger protein 5
PCR	Polymerase chain reaction
PD	Peptidoglycan

PDM	Product of the difference from the mean
PTM	Post-translational modification
qPCR	Quantitative polymerase chain reaction
qRT-PCR	Quantitative reverse transcriptase polymerase chain reaction
RC	Reticulate cell
RNA	Ribonucleic acid
SCF	Skp, Cullin, F-Box containing complex
siRNA	Small interference ribonucleic acid
THP-1	Human acute monocytic leukemia cells
TLR	Toll-like receptor
TRP	Tandem repeat protein
Ub	Ubiquitin; ubiquitinated
Wnt	Wingless-related integration site
WT	Wildtype

Chapter 1. Introduction

***EHRLICHIA CHAFFEENSIS* AND HUMAN MONOCYTOTROPIC EHRLICHIOSIS**

Ehrlichia species are tick borne gram-negative, obligately intracellular bacteria in the family *Anaplasmataceae* within the order Rickettsiales. *Ehrlichia* contains six named species that are known vertebrate pathogens: *E. ruminantium*, *E. canis*, *E. chaffeensis*, *E. ewingii*, *E. muris*, and *E. minasensis* which was first detected in *Rhipicephalus microplus* ticks and recently reported to infect Brazilian cattle [1,175]. In the early 1900s, the discovery of *E. ruminantium* as the etiologic agent of the ruminant disease, heartwater, brought attention to the *Ehrlichia* species, following with identification of several other *Ehrlichia* species as veterinary pathogens [2]. In 1987, *E. chaffeensis* was identified as the etiologic agent of human monocytotropic ehrlichiosis (HME) [3-6]. In addition to *E. chaffeensis* as an emerging human pathogen, other ehrlichial species were also reported to cause human infections across the globe. *E. ewingii* was identified as the etiologic agent of human granulocytic ehrlichiosis mainly in immunocompromised individuals, and *E. canis* and *E. ruminantium* have been reported to cause human infections in South and Central America and South Africa, respectively [176-178]. There have also been reported cases of human infections caused by *E. muris* in Japan and recently another emerging human ehrlichiosis caused by *E. muris* subsp. *eaucلاirensis* in northern U.S [7-10]. *Ehrlichia* species are significant veterinary pathogens, as well as emerging zoonotic pathogens that pose a significant public health threat to humans.

HME is an emerging tick-borne zoonosis, with annual number of reported cases that has increased to 100-200 cases per 100,000 population, though actual incidence of

infection is likely to be much higher due to underreporting and underdiagnosis [65]. Around 40-60% of patients infected with *E. chaffeensis* require hospitalization with a fatality rate of ~1% [34]. Patients are often present with “flu-like” symptoms and an undifferentiated clinical presentation [180,181]. Clinical symptoms usually develop within 1-2 weeks of being bitten by an infected tick [91] and range from mild to severe. Because the HME is difficult to diagnose, delays in diagnosis and treatment can lead to death even in immunocompetent individuals [184-186]. In severe cases of HME, patients can progress to multisystem failure, involving acute respiratory distress syndrome (ARDS) and meningitis [91,181-183]. Approximately half of the individuals who develop HME do not recall being bitten by a tick.

Because of their obligate intracellular existence, *Ehrlichia* species have very limited spectrum of antibiotic susceptibility [187]. Doxycycline is most effective and is the preferred first line of treatment for HME. Therapy should be initiated as soon as there is clinical suspicion of the disease, as this antibiotic is the most effective at preventing disease progression and severe complications when administered within the first week of illness [183]. HME is difficult to diagnose when patients present, however, PCR can confirm the clinical diagnosis before antibodies are detectable [188]. Patients treated within the first five days after presenting with symptoms, typically resolve fever within 24-72 hours [181-183]. However, for patients that progress to more severe symptoms, may require longer hospitalization and time to recover [179,182]. The current standard treatment duration is for at least 3 days after fever has resolved, but for some patients, they may still experience headaches and weakness weeks after treatment [CDC, 179]. Chloramphenicol, a second line of treatment for Rocky Mountain spotted fever (RMSF, a

disease often confused with HME), is not recommended for treating HME due to lack of efficacy [189]. While rifampin is ineffective in treating RMSF, it appears to be effective against *Ehrlichia* in laboratory studies [187]. Treatment for HME is currently only limited to a broad-spectrum antibiotic, therefore, better understanding of the mechanisms *E. chaffeensis* employs to establish infection is necessary for vaccine and targeted therapeutic development.

***EHRLICHIA CHAFFEENSIS* LIFECYCLE**

E. chaffeensis is naturally maintained in a zoonotic cycle involving *Amblyomma americanum* ticks (lone star tick) and a mammalian host that can support a persistent infection, such as the white-tailed deer (*Odocoileus virginianus*) [190,191]. Humans are accidental hosts and only become infected when bitten by an infected tick during the spring and summer when ticks are active [192]. HME is usually transmitted to individuals participating in outdoor activities in areas populated with the lone star ticks [193]. The geographic distribution of the disease is consistent with the distribution of *Amblyomma americanum* and includes southeastern, eastern and north-central to northern U.S. [190,194,195].

E. chaffeensis exhibits tropism for mononuclear phagocytes, and during infection of host cells, the bacterium exists as two ultrastructural forms during its developmental cycle: 1) as infectious dense-cored cells (DC) and 2) as replicative reticulate cells (RC). Both forms of the bacteria reside as microcolonies within the cytoplasmic vacuoles called morulae [11]. Once they enter the mammalian host cells, the morulae have phenotypic markers that resemble early endosomes including presence of Rab5, transferrin, transferrin receptor (TfR), early endosome antigen 1 (EEA1), caveolin 1, GM1

ganglioside and phospholipase Cy2 (PLC- γ 2) [196]. A recent study revealed that late endosomal marker Rab7 is also expressed despite that the ehrlichial vacuoles do not fuse with lysosomes [197]. We recently reported the presence of autophagy markers including LC3, Beclin-1 and p62 on the morula, with increasing levels of LC3II during infection indicating autophagosome formation. However, colocalization of LC3II is not detected with lysosome marker LAMP2, which further confirms that lysosomal fusion and autophagy are inhibited during infection [209]. At 1 h post-infection (hpi), DCs attach to the host cell surface and in the process of being endocytosed into the cytoplasm [11]. Although the exact mechanism is not completely defined, several host proteins and *E. chaffeensis* secreted proteins have been described to facilitate entry. These include the ehrlichial entry triggering protein EtpE, the 120 kDa tandem repeat effector (TRP120), and the host GPI-anchored protein DNase-X [12, 13]. After entry, the ehrlichial life cycle begins and at 1 h post infection (hpi), ehrlichiae transition to intermediate phase-1 (IM1) that proceeds to a complete RC form transition. By 24 hpi, most of *E. chaffeensis* are in RC form, residing within morulae as a single bacterium. The bacteria multiply by binary fission in the RC form until 48 hpi. Between 48-72 hpi, the bacteria transition back to DCs (intermediate phase-2, or IM2). Finally, by 72 hpi, most of *E. chaffeensis* have stopped multiplying and exist as DCs to be released to infect new cells that probably occurs through host cell lysis or exocytosis, but the exact exit mechanism remains undefined [14]. It has been shown that the survival of *E. chaffeensis* depends on the bacterium-secreted effector proteins for: 1) internalization of *E. chaffeensis*, 2) establishment of intracellular infection, and 3) avoiding antimicrobial defenses from host cells [11].

Ehrlichia chaffeensis and other Ehrlichiae have a gram-negative envelope composed of a bacterial outer membrane and inner cytoplasmic membrane, separated by a periplasmic space [198]. However, a unique feature to the family of *Anaplasmataceae* is that the cell wall of these bacteria lacks lipopolysaccharides (LPS) and peptidoglycan (PG), presumably as a measure to evade innate immune responses otherwise elicited by LPS and PG during infection [92, 198]. Despite lacking genes that synthesize LPS and PG, *E. chaffeensis* contains host cholesterol in its outer membrane composition [92]. *E. chaffeensis* requires exogenous cholesterol to maintain structural integrity and infection [92]. *E. chaffeensis* also has relatively small genome size (~1.2Mb) that has lost redundant genes through reductive evolutionary processes, and as a result, many necessary functions of *E. chaffeensis* rely on the host cell machinery [93]. As such, a subset of their gene products is made for host-pathogen interactions, including the secreted tandem repeat proteins (TRPs) and ankyrin repeat proteins [93].

TANDEM REPEAT PROTEINS AND OTHER BACTERIAL MOONLIGHTING EFFECTORS

TRPs are ehrlichial effectors that are secreted via the type I secretion system (T1SS), one of the major secretion systems utilized by *E. chaffeensis*, the other being type IV secretion system (T4SS). The T1SS is a one-step secretion system that allows proteins and other molecules to pass through the inner and outer hydrophobic membranes into the extracellular space. It is also known as ABC-dependent and comprised of three components: an ATP-binding cassette (ABC) transporter (ECH0383), HlyD membrane fusion protein (ECH0970) that is located in the inner membrane, and TolC outer membrane protein (ECH1020) [15-17]. The presence of secretion sequence composed of specific amino acids (LDAVTSIF) in the C-terminus of effectors is necessary for T1SS

recognition [18, 19]. Several *E. chaffeensis* T1SS substrates including TRPs and the 200 kDa ankyrin repeat protein (Ank200) all possess repeat-containing domains of various sizes and sequences [20]. Currently there are four known TRPs described to be secreted by *E. chaffeensis* (TRP32, TRP47, TRP75 and TRP120) [16]. After secretion and through unknown mechanisms, these TRPs are translocated from the morula to various subcellular compartments, including the host nucleus, to interact with a diverse group of proteins to manipulate host cellular processes [16].

Through interactions with the host cell, studies have revealed that TRPs participate in a dynamic range of functions that are important for establishing a favorable environment for infection. They are involved in many different molecular host-pathogen interactions including DNA binding and protein-protein interactions with host substrates important for cell signaling, transcriptional regulation, post-translation modifications (PDM), metabolism, vesicle trafficking and apoptosis [14-16,21,22]. This multifunctional characterization of proteins is called protein moonlighting, and it is often observed in highly conserved proteins in both eukaryotes and prokaryotes [199]. Especially in bacterial pathogens, the protein moonlighting properties have become a major advantage and contribute greatly to their virulence [199]. However, it must be noted that protein moonlighting is complicated in that not all bacterial homologs exhibit protein moonlighting, or not all of them have the same moonlighting functions. One of the earliest evidences of protein moonlighting was discovered in GAPDH of gram-positive group A streptococci. It has been reported that the surface protein of *S. pyogenes* contains sequence homology to other GAPDH and binds to lysozyme, cytoskeletal proteins and fibronectin [94]. Another study reported the same protein also acts as a surface receptor

for plasminogen [95,96]. In addition, *S. pyogenes* GAPDH has been shown to have self-ADP-ribosylating enzymatic activity that contributes to cell invasion, which is an enzymatic process that is utilized by many bacterial toxins [97]. Other streptococci utilize GAPDH for a different purpose, such that in *S. pneumoniae*, GAPDH is observed to bind with plasminogen, important for the pathogen to cross endothelial and epithelial barriers to cause pneumonia and meningitis [98,99].

Enolase is also another prototypic moonlighting protein that is responsible for causing various human diseases as such cancer, chronic autoimmune diseases and Alzheimer's disease [200-203]. Enolase is first identified as carbon-oxygen lyases involved in glycolysis and gluconeogenesis [204]. Later studies have demonstrated additional roles of enolase including neurotrophic factor 14-3-2, heat-shock protein 48 (HSP48) in yeast, hypoxic-stress protein, *MYC* transcription protein, and among others [203-208]. Moreover, this surface protein has been reported to exhibit protein moonlighting properties in many bacteria including both gram-positive and gram-negative pathogens and mostly involved in interaction with plasminogen and fibronectin [100,101]. Moreover, in *Listeria monocytogenes*, the Listeria adhesin protein (LAP) is identified to allow the bacteria to bind to the intestinal epithelial cells and later discovered to bind to the heat shock protein 60 (Hsp60) on the surface of host cells [102,103]. Other bacteria such as *Helicobacter pylori* and *Chlamydia pneumoniae* also secrete moonlighting proteins. The most studied example is the chaperone protein 60 (Cpn60) protein, which is identified as a cell surface protein in *H. pylori* and is involved in cell signaling that contributes to gastric carcinoma oncogenesis, in addition to acting as adhesion for binding to epithelial cells [104,105]. In the intracellular pathogen *C. pneumoniae*, Cpn60

has been reported to play a role in stimulation of monocyte inflammatory cytokine and metalloproteinase synthesis, resulting in accumulation of cytokine levels as a measure to reinforce its pathogenicity [106-108]. In addition to regulating cytokine synthesis, Cpn60 has also been shown to induce oxidation of LDL, TLR4 binding and activation of the MAPK pathway in *C. pneumoniae* infected cells [109,110]. There are many other bacterial moonlighting effectors that play putative roles in bacterial survival and virulence, and in-depth studies still need to be done to fully understand their capabilities to cause infection.

In recent years, our laboratory has made strides in understanding the multifunctional roles of TRPs and we have determined many of those functions. Initially, we have identified the nucleomodulin activities of TRP120 where it enters the nucleus to interact with the host chromatin, and the TR domains are shown to bind to a G+C-rich motif in the host DNA [21]. Moreover, multiple genes involved in host cell transcriptional regulation, signal transduction, and apoptosis are targeted by TRP120 and shown to be upregulated during infection [21, 22]. We have also determined that TRPs are involved in PTMs and facilitation of downstream signaling events such as transglutamination, phosphorylation and phospholipase C γ 2 (PLC- γ 2) activation, inositol 1,4,5-trisphosphate (IP3) production, and calcium release [23-25]. Together, these TRPs are shown to interact with Wnt receptors for Wnt signaling pathway activation to mediate phagocytosis and to facilitate internalization of *E. chaffeensis*. More specifically, TRP120 also directly interacts with Notch and ADAM17 to activate the evolutionarily conserved Notch signaling pathway in order to evade innate immune detection and to promote infection [26]. These investigations clearly show the importance of TRP moonlighting properties in

manipulation of host cellular processes to maintain intracellular survival and promote infection.

OVERVIEW OF BACTERIAL NUCLEOMODULINS AND INTERACTION WITH THE HOST CELLS

As previously mentioned, *E. chaffeensis* TRPs have been shown to act as nucleomodulins. Nucleomodulins are part of an emerging group of bacterial effectors that function within the host cell nucleus in activities including regulation of host gene expression and other processes. Studies of the nucleomodulin functions have led to deeper understanding of the mechanisms which the pathogens through nucleomodulins activity promote infection.

The earliest nucleomodulin was discovered in the plant pathogen *Agrobacterium tumefaciens*, that integrates its tumor-inducing (Ti) plasmid to genetically modify the plant genome. The result is generation of tumor cells that serve as nutrient production factory for the bacteria [111]. Further discoveries of phytopathogen nucleomodulins were made in the 2000s and founded an interest in nucleomodulins secreted by human or other animal pathogens. In the last decade, emerging studies have reported the ability of human pathogens to function inside host cell nucleus and the number of recognized nucleomodulins is increasing along with understanding of their sophistication and complexity. For example *Listeria monocytogenes*, a causative agent of listeriosis, secretes *Listeria* nuclear targeted protein A (LntA) to bind to human BAHD1 protein in the host cell nucleus to repress expression of interferon lambda [112,113]. A second nucleomodulin, OrfX, has been discovered among other virulent *L. monocytogenes* proteins [114]. It is identified to interact with host multifunctional zinc finger nuclear

protein (RYBP) with many other transcription factors and co-factors [115]. In addition, OrfX decreases the level of RYBP by regulating the production of ROS through manipulation of E3 ubiquitin ligase MDM2-p53 pathway [115,116].

Nucleomodulins have also been shown to act as chromatin-modification enzymes, including *Chlamydia trachomatis* nuclear effector NUE [117]. It is identified to function as a lysine methyltransferase for host histones H2B, H3 and H4, although additional studies are needed to explore its target genes [118,119]. Similarly, RomA/LegAS4, a T4SS effector secreted by *Legionella pneumophila*, was discovered to be a histone methyltransferase [120]. Depending on its intranuclear localization, RomA/LegAS4 can modify different histones and activate expression of rRNA, specifically by targeting the rRNA promoter and intergenic regions through interaction with HP1 α/γ [121]. Another nucleomodulin that modifies host chromatin is Rv1988 of *Mycobacterium tuberculosis*, which is responsible for the reduction of ROS activity in macrophages via dimethylating an arginine residue in histone H3 to repress expression of *NOX1/4* [122]. Other pathogens use nucleomodulins to manipulate PTMs to modify host chromatin, such as OspF of *Shigella flexneri*, that permanently modifies a threonine residue on MAPK to prevent its phosphorylation and results in sequestration of the protein in the nucleus, ultimately inhibiting phosphorylation of histone H3 and downstream expression of pro-inflammatory genes [123].

Beside interaction with host chromatin to regulate downstream transcription, these bacterial nucleomodulins also function to disrupt host cellular processes through regulation of host proteins. For example, *S. enterica* serovar Typhimurium produces a

group of metalloproteases (PipA, GogA and GtgA) to degrade NFkB subunits, resulting in repressed inflammatory response [137,138].

Protein-protein interactions are often observed between proteins with domains containing repeats. The most common repeat is the ankyrin repeats (Ank) seen in many gram-negative pathogens including *Rickettsia*, *Ehrlichia*, *Anaplasma* and *Coxiella* [139]. *E. chaffeensis* secretes an Ank repeat-containing protein (Ank200) and a group of tandem repeat proteins (TRPs) that reprogram the host cell. To date, Ank200 and the four known TRPs (TRP32, TRP120, TRP47 and TRP75) are all characterized to be nucleomodulins [16]. Ank200 has been shown to bind to chromatin at AT-rich DNA regions to downregulate target genes involved in a dynamic range of functions including transcriptional/translation regulation, cell signaling, intracellular trafficking, immune response and cytoskeletal rearrangement [140]. In addition to Ank200, TRP32 and TRP120 have also been demonstrated to interact with host DNA at G-rich and G+C rich motifs, respectively, and bind with various chromatin-remodeling complexes including polycomb-group (PcG) proteins [21]. Recently, we have reported that TRP47 interacts with host DNA at G+C rich motifs to target multiple genes [141]. Furthermore, *E. chaffeensis* TRPs are also known to engage in protein-protein interactions that encompass a myriad of cellular processes including immune response, cell signaling, cell proliferation/differentiation, and apoptosis. Not only does TRP120 function as a nucleomodulin to interact with host DNA and mimic host ligand to activate major signaling events, we have shown that TRP120 acquire PTMs from host cell machinery and also capable of acting as a ubiquitin ligase. Notably, TRP120 itself is post-translationally modified, such that TRP120 SUMOylation occurs at a canonical

consensus SUMO motif, IKEE. SUMOylation of TRP120 enhances interactions with several host proteins including γ -actin and PCGF5 [27-28]. In addition to SUMOylation, TRP120 is also described to function as a HECT E3 Ub ligase [29]. Likewise, *S. flexneri* and other pathogens including *Salmonella enterica* and *Yersinia* spp. have been shown to secrete nucleomodulins that also function as E3 ubiquitin ligases, such as IpaHs, SspH1 and YopM, respectively [124-131].

BACTERIAL UBIQUITIN LIGASES

Many of the nucleomodulins secreted by human pathogens function as E3 Ub ligases. E3 Ub ligases are integral enzymes that transfer ubiquitin to a substrate as part of the PTM system. PTMs are utilized by the cells to regulate downstream gene expression and cell signaling, manipulation of the ubiquitination system is a method which several bacteria are employing to promote their survival and infection. *Shigella flexneri* secretes a family of effectors, IpaHs, that were recently identified as E3 ubiquitin ligases [124,125]. These effectors engage both host nuclear and cytosolic proteins resulting in ubiquitination and proteasomal-dependent degradation, including host splicing factor U2AF35 as a nuclear substrate for IpaH9.8 [126,127]. *S. flexneri* IpaHs contain a leucine-rich repeat domain (LRR) in the N-terminus that functions as substrate recognition domain, and the E3 ligase domain called NEL in the C-terminus [128,129]. This NEL domain is also found in *Salmonella enterica* SspH1, which has been shown to target host PKN1 kinase for degradation to inhibit NF κ B-dependent pro-inflammatory genes [130]. In addition to SspH1, *S. enterica* SopA has been characterized to contain a HECT-domain and demonstrated to have E3 Ub ligase activity [142,143]. Similar to *Shigella* IpaH and *Salmonella* SspH1, *Yersinia* spp. YopM is characterized as a scaffolding

protein of an E3 ubiquitin ligase complex that targets RSK1 and PKN2 [131-133]. In addition, *E. coli* nucleomodulin NleG5-1 contains an Ub ligase U-box domain and functions as an E3 ligase to degrade host MED15 in the nucleus to downregulate transcription [134]. A recent study has demonstrated that *Orientia tsutsugamushi* produces a family of Ank proteins that contain a F-Box-like domain in the C-terminus [135]. They have been shown to interact with the human SKP1 and CUL1 of the SCF E3 Ub ligase complex to promote degradation of substrates, one of the substrates appears to be transcription factor EF1-alpha [136].

Another bacterial effector that manipulates the SCF Ub ligase complex, and the focus of this project, is *E. chaffeensis* TRP120. Recently, our laboratory discovered that TRP120 contains a HECT (homologous to the E6-AP carboxyl terminus) domain in the C-terminus with an active cysteine that is required for transferring ubiquitin onto the substrate [29]. Further investigation has shown TRP120 exhibits ubiquitin ligase activity on a substrate known as polycomb group ring finger protein 5 (PCGF5), suggesting TRP120 plays an important role in ubiquitination of host cell substrates as another method to manipulate host cellular processes [29]. The initial Y2H study has indicated ~100 host proteins can interact with TRP120, many of which are involved in host cell signaling pathways for cell differentiation, proliferation and apoptosis. In this project, FBW7, one of the TRP120 binding partners was explored in depth and we have determined that FBW7 is indeed a substrate of TRP120 Ub E3 ligase activity.

TUMOR SUPPRESSOR FBW7

FBW7 is short for F-Box and WD repeat domain-containing 7, which is the substrate recognition subunit of the evolutionarily conserved SCF (SKP1, CUL1 and F-Box) E3

Ub ligase complex [21]. FBW7 was originally discovered in a budding yeast, called Cdc4, and it later became apparent that this protein controls cell cycle through regulating cyclin-dependent kinase inhibitor Sic1 in yeast [144,145]. Additional studies have further characterized that phosphorylated Sic1 binds to Cdc4 (FBW7) at a conserved motif later coined as the Cdc4 phospho-degron (CPD) [146]. From that point forward, multiple investigations have led to the discovery of human Cdc4 orthologue, FBW7, along with the identification of Notch1 and Cyclin E being its substrates [147-149]. Human *FBW7* gene is over 200 kb and through alternatively splicing, three isoforms (*FBW7* α , β and γ) are produced [150]. Although the three isoforms are functionally identical, they are differentially regulated and expressed in distinct subcellular compartments [150]. For example, *FBW7* α is expressed ubiquitously in most human cell types at high levels, whereas *FBW7* β and *FBW7* γ are detected only in the brain and muscles, respectively [151]. For the purpose of this project, considering the host cell of *E. chaffeensis*, *FBW7* α was investigated.

All three *FBW7* isoforms are functionally identical but occupy distinct subcellular compartments due to differences found in the N-terminal domain [152]. *FBW7* α (*FBW7*) is observed in the nucleoplasm, *FBW7* β is directed to the cytoplasm, and *FBW7* γ is only present in the nucleolar [153]. *FBW7* protein has three conserved domains for protein-protein interaction. The F-Box domain is for recruiting and interacting with SKP1 of SCF E3 Ub ligase complex, the second domain is a stretch of WD40 repeats that recognizes phosphorylated substrates and the repeats allow multiple contacts with the substrates [154,155]. The third domain is the D domain or Dimerization domain, allows dimerization of *FBW7* within the SCF complex [156]. Studies have shown that

dimerization of FBW7 allows a stronger interaction with its substrates as well as addition of the polyubiquitins for degradation, although this appears to be strongly dependent on the degron strength since monomeric FBW7 can efficiently degrade cyclin E [156-158].

The substrates of FBW7 are well characterized and have a broad range of functions. Substrates of FBW7 include Notch, cJun, cMYC, Notch, MCL1 and cyclin E. These proteins are also widely studied in the field of cancer biology and are known oncoproteins, therefore making FBW7 a tumor suppressor. Notably, FBW7 appears to play a crucial role in regulating the Notch signaling pathway by targeting both upstream Notch activator presenilin and downstream protein cMYC [159-161]. Unsurprisingly, *FBW7* is located within 4q32, a common chromosome region that often gets deleted in cancers [162]. The loss of function of FBW7 leads to an increase in oncoprotein levels and subsequent tumorigenesis.

While regulation of FBW7 substrates has been well-studied, the regulation of FBW7 itself has been overlooked in the past. Emerging evidence has shown FBW7 is transcriptionally regulated by various proteins including p53, Pin1, C/EBP- δ , Hes5 and Numb, and by microRNAs such as miR-27a and miR-223 [163-165]. Furthermore, studies have shown FBW7 is also post-translationally modified, such that phosphorylation of FBW7 at Ser10 and Ser18 controls its subcellular localization [166]. In addition, phosphorylation at Ser205 recruits Pin1 to FBW7 and promotes binding and autocatalytic ubiquitination to facilitate FBW7 turnover [167]. However, additional studies are needed to further explore the mechanisms by which FBW7 is regulated.

PROJECT INTRODUCTION

E. chaffeensis secreted effector, TRP120, has been shown to interact strongly with ~100 host cell proteins, with a diverse array of functions including transcription regulation, metabolism, post-translational modifications and cell signaling regulation [22]. This discovery has opened the doors to explore the interactions of TRP120 with different host binding partners and has since become a main focus in our laboratory. We have used this information to generate mechanistic hypotheses to better understand ehrlichial pathobiology. Hence, our previous studies led to this investigation to understand the role of TRP120-FBW7 interaction as it relates to Notch signaling pathway to promote infection. This study has provided further evidence that intracellular survival requires ehrlichial manipulation that results in regulation of host cell signaling events [26]. In addition, we have recently determined that TRP120 contains a HECT-like E3 ligase domain that targets interacting host proteins for ubiquitin (Ub)-mediated degradation [29]. One of the host proteins that TRP120 interacts with is the tumor suppressor F-box and WD40 repeat domain-containing 7 (FBW7), a substrate recognition subunit of the host E3 ligase complex SCF (Skp1, Cul1, F-box) that is regulated through autoubiquitination [22, 30, 31]. It has also been well described that FBW7 functions as a negative regulator for several oncoproteins including Notch [32]. Moreover, we have shown that the knockdown of FBW7 also leads to significantly increased ehrlichial infection [22]. However, whether TRP120 interaction with FBW7 involves ubiquitin ligase activity of the bacterial effector, and the role that this interaction plays in maintaining Notch signaling activation during infection remain unclear. This information established the premise to support my hypothesis that *E. chaffeensis* TRP120

ubiquitinates FBW7 for degradation and results in the maintenance and amplification of Notch signaling and other downstream pro-survival proteins to promote infection.

The objective of this project is to determine the molecular details that are necessary for the interaction and identify FBW7 as a substrate for TRP120 ubiquitin ligase activity, and to demonstrate that *E. chaffeensis* TRP120-driven ubiquitination-dependent degradation of FBW7 leads to stabilization and upregulation of downstream pro-survival proteins. Three aims were originally proposed to test this hypothesis. **Aim 1** was to determine the FBW7-TRP120 interacting domains. **Aim 2** was to investigate the role of TRP120-mediated ubiquitination in FBW7 degradation. **Aim 3** was to determine the role of FBW7 degradation in stabilization and amplification of downstream FBW7 targets to promote ehrlichial infection. The findings of my research have led me to conclude that FBW7 is a new TRP120 substrate and is targeted for ubiquitination and subsequent degradation in order to promote infection through stabilization of pro-survival proteins (Notch, c-Jun, MCL1 and cMYC). We further determined that the ubiquitin ligase activity is another of the many TRP120 nucleomodulin functions.

Chapter 2. Materials and Methods

Cell culture. Human monocytic leukemia cells (THP-1) were grown and maintained in RPMI medium 1640 with L-glutamine and 25 mM HEPES buffer (Invitrogen, Carlsbad, CA), supplemented with 10% fetal bovine serum (HyClone, Logan, UT). Henrietta Lack's cervical epithelial adenocarcinoma (HeLa) cells were propagated in MEM medium with Earle's Salts and L-glutamine (Thermo Fisher Scientific, Waltham, MA), supplemented with 10% fetal bovine serum (HyClone). *E. chaffeensis* (Arkansas strain) was cultivated in THP-1 cells as previously described [25].

Cell lysis and protein extraction. *E. chaffeensis*-infected THP-1 cells were harvested at 24, 48 and 72 h post infection (hpi), and whole-cell lysates (uninfected THP-1 cells were used as controls) were extracted three times in complete-RIPA buffer supplemented with cOmplete Protease Inhibitor Cocktail tablet (Sigma-Aldrich, St. Louis, MO) and Halt Phosphatase Inhibitor Cocktail (Thermo Fisher Scientific). Lysates were centrifuged at 13,000 x g for 30 s to pellet insoluble material and cleared by centrifugation at 13,000 x g for 20 min at 4°C. The protein concentration was determined using Pierce BCA Protein Assay (Thermo Fisher Scientific). In addition, equal mass amount of N-ethylmaleimide (NEM; Thermo Fisher Scientific) was added to the whole cell lysates to preserve native ubiquitination of proteins in co-immunoprecipitation experiment performed for Figure 4A. Lastly, for the western blot experiment in Figure 4B, 26S proteasome inhibitor, Bortezomib (Thermo Fisher Scientific), was added to cell culture at 10ng/ml concentration for 10 h before whole cell lysates were collected.

RNA extraction, cDNA synthesis and qRT-PCR. Total RNA from *E. chaffeensis*-infected and uninfected THP-1 cells was isolated with the RNeasy Mini Kit (Qiagen,

Beverly, MA) using on-column DNA digestion with RNase-free DNase reagent (Qiagen). cDNA synthesis was performed with total RNA (1 µg) using qScript cDNA Synthesis Kit (Quantabio, Beverly, MA). Quantitative real-time PCR was performed with iQ SYBR Green SuperMix (Agilent Technologies, Santa Clara, CA) with gene-specific primers. Forward FBW7: 5'-CCACTGGGCTTGTACCATGTT-3'; reverse FBW7: 5'-CAGATGTAATTCGGCGTCGTT-3'. Forward GAPDH: 5'-GCTCTCTGCTCCTCCTGTTC-3'; reverse GAPDH: 5'-TTCCCGTTCTAGCCTTGAC-3'.

RNAi and quantification of *E. chaffeensis* by qPCR. Specific FBW7 siRNAs were siGENOME SMARTpool siRNA (Dharmacon, Lafayette, CO), which are endoribonuclease-prepared siRNA pools containing heterogenous mixture of four different siRNAs targeting the same human FBW7 mRNA sequence. The control siRNA was ON-TARGET_{plus} non-targeting siRNA (Dharmacon) designed to have fewer off-targets than standard unmodified negative control siRNAs. Quantification of *E. chaffeensis* by qPCR after RNA interference has been previously described [33].

Confocal immunofluorescent microscopy. THP-1 cells were plated in 6-well plates and infected with cell-free *E. chaffeensis* at a multiplicity of infection (MOI) of 100 for 24, 48 and 72 h. Cells were cytocentrifuged onto glass slides and fixed in ice-cold 4% paraformaldehyde in PBS for 20 min then permeabilized and blocked in 1% Triton-X 100 in PBS with 5% bovine serum albumin for 1 h. The cells were incubated with rabbit anti-TRP120 peptide antisera (1:1000) and mouse anti-FBW7 monoclonal antibody (1:100; R&D Systems, Minneapolis, MN) for 1 h, washed three times with PBS and incubated with anti-rabbit Alexa Fluor 488-IgG (H+L) and anti-mouse Alexa Fluor 594-IgG (H+L)

secondary antibodies for 1 h. Slides were washed three times with PBS and mounted with ProLong Gold Antifade reagent with 4',6-diamidino-2-phenylindole (DAPI; Invitrogen). Images were obtained using a Zeiss Laser Scanning Microscope 880 with Airyscan and processed using Zeiss ZEN Microscopy Software (ZEISS, Oberkochen, Germany) and FIJI (An acronym for FIJI Is Just ImageJ).

Generation of FBW7 and TRP120 constructs, and recombinant TRP120. FBW7 truncation gene constructs (FBW7-N, FBW7-FBOX, and FBW7-WD40) were created using PCR amplification from pGEM-FBW7 plasmid (Sino Biological, Wayne, PA) and cloning into the pcDNA3.1/His mammalian expression vector (Thermo Fisher Scientific). Plasmid DNA of FBW7-N, FBW7-FBOX and FBW7-WD40 clones was obtained from transformed TOP10 *E. coli* cultures and purified using QIAprep Spin Maxiprep kit (Qiagen). Full-length FBW7 plasmid was purchased as pcDNA3.1+/C-(K) DYK-FBW7 (GenScript, Piscataway, NJ). The same FBW7 domain constructs were also used for purification from HeLa cells through immunoprecipitation to obtain recombinant proteins used in co-IP experiment (Fig. S1). Full length and tandem repeat-C-terminal domain (TR-C) and mutant plasmids with cysteine to serine point mutations at the C-terminus (C520S) of TRP120 were gene synthesized and cloned into pcDNA3.1+C-eGFP (GenScript). Recombinant TRP120-His used for in vitro ubiquitination experiments was purified from TOP10 *E. coli* transformed with pBAD/TOPO-Thio-TRP120 plasmid as previously described [21, 28]. Recombinant TRP120-TR-GST used for co-IP experiment (Fig. S1) was purified using glutathione Sepharose 4B (GE) from *E. coli* BL21 cells transformed with pGEX-6p1-TRP120-TR plasmid.

Transfection and immunofluorescent microscopy. The plasmid DNA was transfected into HeLa cells using Lipofectamine 2000 (Invitrogen) according to manufacturer's protocol. Cells ectopically expressing TRP120 or FBW7-His were cytocentrifuged onto glass slides and fixed in ice-cold 4% paraformaldehyde in PBS for 20 min then permeabilized and blocked in 1% Triton-X 100 in PBS with 5% bovine serum albumin for 1 h. The cells were incubated with rabbit anti-TRP120 (1:1000) and mouse anti-His antibodies (1:100) at room temperature for 1 h, then washed and incubated with anti-rabbit Alexa Fluor 488-IgG (H+L) and anti-mouse Alexa Fluor 594-IgG (H+L) secondary antibodies for 1 h. Images were obtained using an Olympus BX61 epifluorescence microscope and analyzed using SlideBook 6 Reader software (Intelligent Imaging Innovations, Denver, CO) and FIJI.

Quantitative microscopy and Mander's overlap coefficient (MOC).

Quantification of immunofluorescence microscopy and calculation of Mander's coefficient were carried out using WCIF-ImageJ (Bob and Joan Wright Cell Imaging Facility, Krembil Research Institute), which contains plugin for intensity correlation analysis (ICA) and corrected total cell fluorescence (CTCF). ICA was used to calculate Mander's overlap coefficient (MOC) by using the selection tool to mark the regions of interest. Similarly, CTCF values were collected using the measurement tool after the selection of the regions of interest in a micrograph.

***In vitro* precipitation of recombinant TRP120 and FBW7.** Recombinant TRP120-GST was incubated at 4°C overnight with recombinant FBW7-His or recombinant WD40-His in native equilibration buffer (50 mM NaH₂PO₄, 300mM NaCl, pH=7.0). All proteins were also incubated alone as control. Samples were placed onto cOmplete™

His-Tag Purification Resin (Sigma-Aldrich) to immobilize the His-tagged bait from the samples overnight at 4°C. Unbound protein was washed away with equilibration buffer containing 5mM, 10mM, or 20mM Imidazole. Protein-protein interaction complexes were eluted using equilibration buffer containing 500mM imidazole. Western blot analysis was performed on eluted samples. Detection of FBW7 and WD40 was performed with anti-His antibody and TRP120 was detected using both anti-TRP120 and anti-GST antibody.

Co-immunoprecipitation and Western immunoblot. Co-immunoprecipitation (co-IP) was performed with 3-day post-infection (95-100%) THP-1 cells using Pierce Protein A/G Agarose kit (Thermo Fisher Scientific) according to manufacturer's protocol. Protein samples were resolved by SDS-PAGE, transferred onto nitrocellulose membranes, and blocked for 1 h at room temperature in Tris-buffered saline with 5% nonfat dry milk and 1% Triton-X 100. Primary antibodies included mouse anti-FBW7 (1:1000; R&D Systems, used to detect both unmodified and ubiquitinated FBW7), rabbit anti-TRP120 peptide antisera (1:10,000), rabbit anti-GAPDH (1:10,000; Proteintech, Rosemont, IL), rabbit anti-NICD (1:1000; Cell Signaling Technology, Danvers, MA), rabbit anti-p-c-Jun (1:1000; Cell Signaling Technology), rabbit anti-MCL1 (1:1000; Cell Signaling Technology), rabbit anti-K48 linkage-HRP conjugated (1:1000; Cell Signaling Technology), mouse anti-FK2 (1:500; Cell Signaling Technology), and mouse anti-cMYC (9E10) (1:500, Santa Cruz Biotechnology, Dallas, TX). Secondary antibodies included horseradish peroxidase-labeled goat anti-rabbit IgG and anti-mouse IgG (1:20,000; Kirkegaard & Perry, Gaithersburg, MD). Densitometry was performed using ImageJ software.

***In vitro* FBW7 ubiquitination assay.** All *in vitro* ubiquitination assays were performed with a Ubiquitinylation kit (Enzo Life Sciences, Farmingdale, NY). FBW7 ubiquitination was performed using purified recombinant TRP120 and native or recombinant FBW7. FBW7 (100 nM) was added to a ubiquitination reaction containing Ub, ATP, inorganic pyrophosphatase and Mg²⁺ (buffer) in presence of E1, UbcH5b E2 and TRP120 (10 nM) as the E3. Negative control reaction did not contain ATP. The assay was performed according to manufacturer's protocol. Ubiquitination reaction was performed at 37°C for 4 h, and the reaction was stopped with the addition of Laemmli buffer. The samples were boiled for 5 min and resolved by SDS-PAGE for Western blot analysis using anti-FBW7, anti-TRP120, and anti-K48 antibodies.

Statistical analysis. The results were evaluated using two-tailed Student t-test with *p*-values of <0.05 considered statistically significant.

Chapter 3. *Ehrlichia chaffeensis* TRP120-Mediated Ubiquitination and Proteasomal Degradation of Tumor Suppressor FBW7 Increases Oncoprotein Stability and Promotes Infection

INTRODUCTION

Ehrlichia chaffeensis (*E. chaffeensis*) is an obligately intracellular, gram-negative bacterium that exhibits tropism for mononuclear phagocytes and resides in microcolonies within membrane-bound cytoplasmic vacuoles known as morulae [34, 35]. *E. chaffeensis* survival in the mononuclear phagocyte is dependent in part on pathogen-host interactions involving tandem repeat protein (TRP) effectors that are secreted via the type-1 secretion system and interact with a diverse array of host targets [14, 22, 24]. TRPs translocate across the morula membrane via an unknown mechanism and enter the host cell cytosol and nucleus where they function to reprogram the cell through direct interactions with well-defined and lesser known host cell targets [22].

One of the most studied *E. chaffeensis* effectors is TRP120, a moonlighting effector that has several defined functions. Early studies demonstrated that surface expressed TRP120 plays a role in host cell entry, but once ehrlichiae are internalized, TRP120 rapidly (<3 h) translocates to the host cell nucleus where it functions as a nucleomodulin, interacts with chromatin-associated proteins and directly binds genes associated with transcriptional regulation, signal transduction and apoptosis [13, 21, 28, 36]. TRP120 is also a functional HECT E3 ligase that ubiquitinates host cell substrates including a

Portion of this chapter is contained in the manuscript titled “*Ehrlichia chaffeensis* TRP120-mediated ubiquitination and proteasomal degradation of tumor suppressor FBW7 increases oncoprotein stability and promotes infection” published by *PLOS Pathogens*, 2020.

known interacting partner, polycomb group ring finger protein 5 (PCGF5), a member of the polycomb repressive complex [29]. TRP120 itself exploits host cell post-translational machinery and is SUMOylated at a canonical motif, which is known to affect TRP120-host target interactions [27, 28].

There is a large group of functionally diverse host proteins that interact with TRP120, including FBOX with WD40 repeat 7 (FBW7), a subunit of the eukaryotic Skp1, Cul1, and FBOX protein (SCF) E3 ligase complex [21, 22, 37]. FBW7 is an evolutionarily conserved tumor suppressor and a member of the FBOX family proteins that constitute the substrate recognition subunit of SCF ubiquitin ligase complex [32]. SCF complex targets a network of well-known oncoproteins (NICD, c-Jun, MCL1, cMYC and cyclin E1) for degradation that are involved in cell proliferation, differentiation and regulation of apoptosis [32, 38]. FBW7 contains two primary domains, the FBOX which binds to Skp1 in the SCF complex, and the WD40 domain that recognizes and binds phosphorylated substrates at a conserved Cdc4 phospho-degron motif [38, 39]. FBW7 self-regulates through phosphorylation-dependent autoubiquitination, in turn affecting the stability of FBW7 target substrates [30, 31]. Interestingly, knockdown of FBW7 leads to a significant enhancement of *E. chaffeensis* infection [22]. Although the role of the TRP120-FBW7 interaction in ehrlichial pathobiology remains to be determined, these findings suggest that FBW7 may be a substrate of TRP120 HECT E3 ligase activity.

Recently, our laboratory reported that the *E. chaffeensis* TRP120 effector is able to activate Notch signaling, which appears to be critical for establishment and maintenance of intracellular infection in human monocytes [26]. However, the role of Notch signaling, and the mechanisms involved in maintaining Notch activation during infection are not

well understood. Notch is an evolutionarily conserved cell signaling pathway that regulates cell proliferation, differentiation and survival [40, 41]. Established functions of Notch signaling in the immune systems include regulating B and T cell differentiation, activation of T helper cells, and participation in regulatory functions of T cells [42-46]. Lesser known, but recognized roles of Notch signaling in innate immune system function, include regulation of toll-like receptor (TLR) expression, induction of inflammatory cytokines in response to viral and bacterial infections, and regulation of apoptosis [42, 47, 48]. However, the exploitation and regulation of Notch signaling pathway by intracellular pathogens has not been described previously.

In this investigation, we have characterized a novel nuclear interaction between the *E. chaffeensis* TRP120 effector and the tumor suppressor FBW7. The interaction ultimately enables the *E. chaffeensis* TRP120 HECT Ub ligase to engage FBW7 as a substrate to initiate a degradation process that involves K48 ubiquitination and proteasomal degradation. The degradation of FBW7 during ehrlichial infection increases Notch intracellular domain (NICD) levels and stabilizes other prominent FBW7-regulated oncoproteins resulting in ehrlichial infection enhancement. This study provides further insight into how evolutionarily conserved signaling pathways are hijacked by obligately intracellular pathogens.

RESULTS

E. chaffeensis TRP120 interacts with human SCF ligase FBW7.

Our laboratory reported an interaction between TRP120 and FBW7 with yeast-two hybrid analysis [22, 33], but this interaction was not fully investigated or confirmed using other approaches. In order to explore the preliminary yeast two-hybrid results, confocal immunofluorescent microscopy was performed to demonstrate nuclear colocalization of TRP120 with FBW7 in *E. chaffeensis*-infected THP-1 cells (Fig. 1A). In the control cells, FBW7 was primarily observed in the nuclei and diffusely distributed throughout the

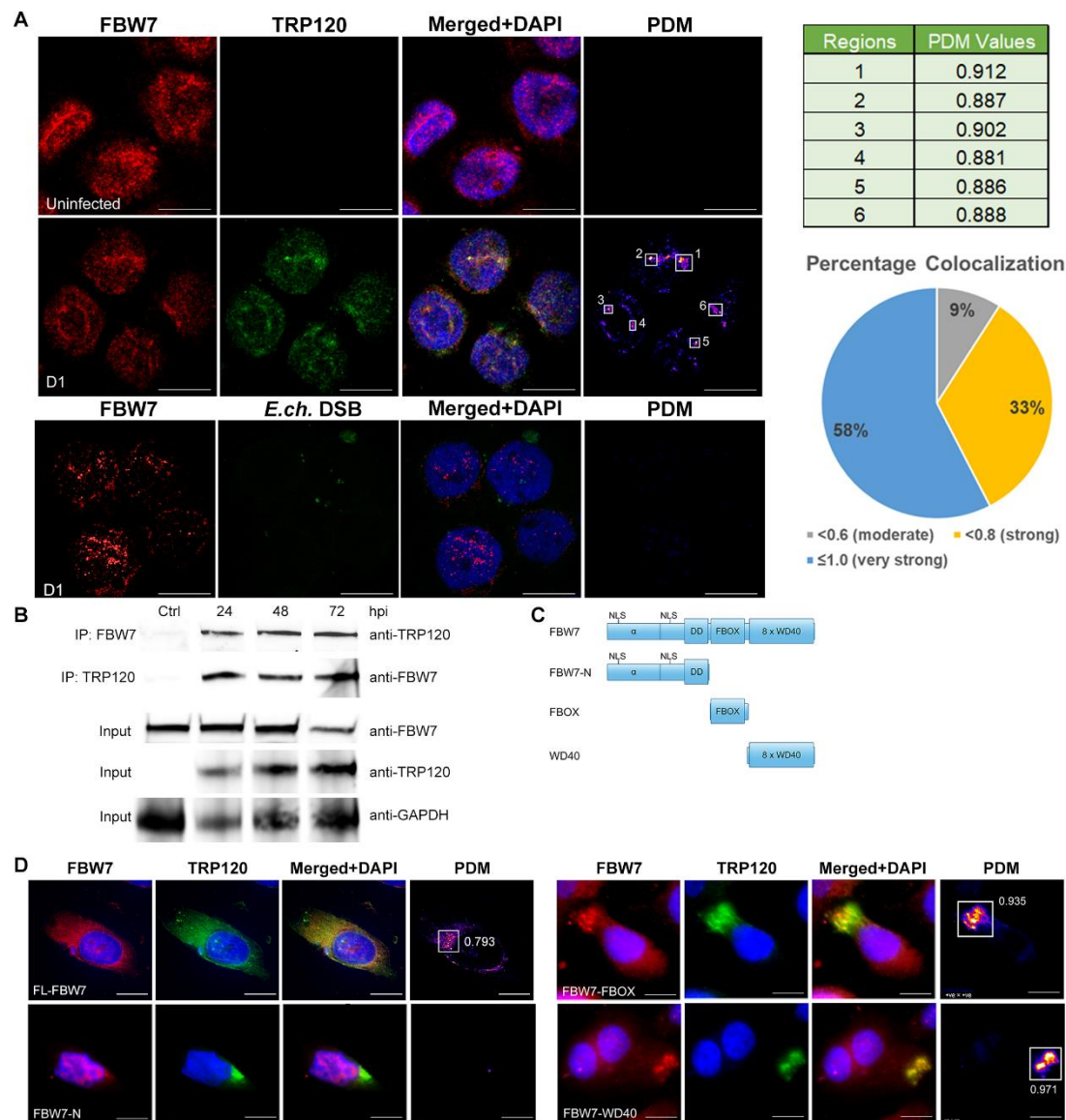


Figure 1: *E. chaffeensis* TRP120-FBW7 nuclear colocalization and interaction with FBW7 FBOX and WD40 domains.

A. Confocal immunofluorescent microscopy demonstrating colocalization of FBW7 (red) and *E. chaffeensis* TRP120 (green) in THP-1 cell nuclei at 24 h post-infection (hpi). Nucleus was stained with DAPI (blue). Confocal immunofluorescent microscopy was performed to further demonstrate FBW7 (red) did not colocalize with *E. chaffeensis* Dsb (green), suggesting specificity of TRP120-FBW7 nuclear colocalization. Colocalization intensity was determined by Product of the Differences from the Mean (PDM) calculation and shown in the heatmap-like image. The brightest points of colocalization in the PDM image were quantified with Mander's overlap coefficients (MOC), which ranges between 0 (no colocalization) to 1 (strong colocalization). A table showing MOC values of the highlighted regions of interest are shown in the *E. chaffeensis*-infected cells (top). In addition, a pie chart was generated from MOC values of multiple regions showing colocalization of TRP120 and FBW7 in the nucleus, where five images (n=5) containing a total of 33 regions (n=33) were analyzed, where 58% have very strong colocalization and 33% have strong colocalization. **B.** Co-immunoprecipitation was performed to demonstrate direct interaction between TRP120 and FBW7. THP-1 cells were infected with cell-free *E. chaffeensis* and then harvested at 24, 48, and 72 hpi. Anti-TRP120 and anti-FBW7 antibodies were first combined with whole cell lysates for coupling to form antigen-antibody complex. A/G coated magnetic beads were added to the antigen-antibody complex to allow binding and pull down of either TRP120 or FBW7. Western immunoblots were probed with anti-FBW7 or anti-TRP120 (n=3). **C.** Schematic representation of truncated FBW7 mutant constructs (His-tagged) generated for ectopic expression experiments. **D.** HeLa cells were co-transfected with FL-FBW7 or FBW7 truncated constructs, and TRP120 to examine colocalization by immunofluorescent microscopy. Colocalization was not observed between TRP120 (green) and FBW7-N (red), but strong colocalization between TRP120 and both FBOX and WD40 domains of FBW7 was detected and colocalization strength shown by Mander's coefficients of 0.935 and 0.971, respectively. This figure was representative of three experiments (n=3) with technical replicates (n=2).

cytoplasm. However, in *E. chaffeensis*-infected cells, FBW7 was only observed in the nucleus in punctate distribution colocalizing with TRP120. Furthermore, intensity correlation analysis was achieved with the Product of the Differences from the Mean (PDM) where the intensities of green and red fluorophores (TRP120 and FBW7, respectively) were calculated. The brightest points of colocalization were also quantified using Mander's coefficients (0→1, 1 is highest colocalization) with an 58% of total analyzed regions of interest with >0.8, indicating a very strong colocalization correlation

between TRP120 and FBW7. We also determined the nuclear colocalization of TRP120 with FBW7 is specific with confocal microscopy demonstrating that FBW7 does not colocalize with *E. chaffeensis* Dsb (disulfide bond formation), a protein that is observed in the periplasm of *E. chaffeensis* (Fig. 1A). In addition, co-IP was used to confirm interaction between TRP120 and FBW7 (Fig. 1B). *E. chaffeensis*-infected THP-1 cells were harvested at 24, 48 and 72 hpi, and TRP120 and FBW7 were independently immunoprecipitated and detected by Western immunoblot analyses. Using co-IP, we found high levels of FBW7 bound to TRP120 in the infected THP-1 cells compared to uninfected controls. Conversely, we observed high levels of bound TRP120 in FBW7 co-IP samples. Immunofluorescent confocal microscopy, ectopic expression, and co-IP analyses demonstrated colocalization and interaction between TRP120 and FBW7, confirming our previous Y2H results.

TRP120 interacts with the FBOX and WD40 domains of FBW7.

FBW7 contains two major domains required for proper function within the SCF E3 ligase complex: Skp1 binding domain FBOX, and substrate recognition/binding domain WD40 [29]. In order to identify the FBW7 domain interacting with TRP120, dual ectopic expression was performed with TRP120 and FL-FBW7 (Full length FBW7), FBW7-N (N-terminus and dimerization domain), FBW7-FBOX (FBOX domain only), and FBW7-WD40 (WD40 domain with complete C-terminus) (Fig. 1C). Co-transfection of TRP120 and the FBW7 truncated constructs was performed in HeLa cells for ectopic expression to visualize colocalization. While TRP120 does not translocate into the nucleus when ectopically expressed, immunofluorescent microscopy revealed FBW7-N was only observed in the nucleus and there was no colocalization observed with TRP120-GFP

(Fig. 1D). However, based on the DNA sequence alignment obtained from Y2H results, TRP120 was found to bind to both FBOX and WD40 domains of FBW7. This was further supported by *in vitro* pull-down of recombinant TRP120-GST with FBW7 domain constructs (FBOX-His and WD40-His) where both domains were shown to be bound to TRP120 (Fig. 2). In ectopic expression experiments, both FBW7-FBOX and FBW7-WD40 constructs colocalized with TRP120-GFP. Furthermore, the PDM images

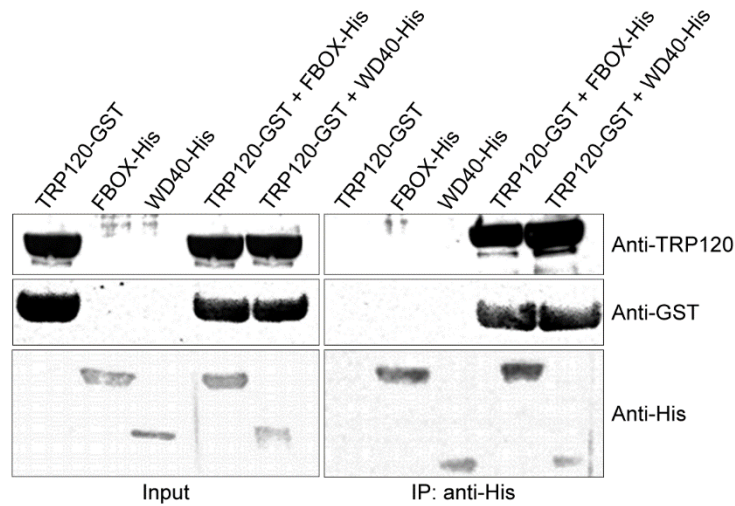


Figure 2: Direct interaction between TRP120-TR with FBW7 domains.

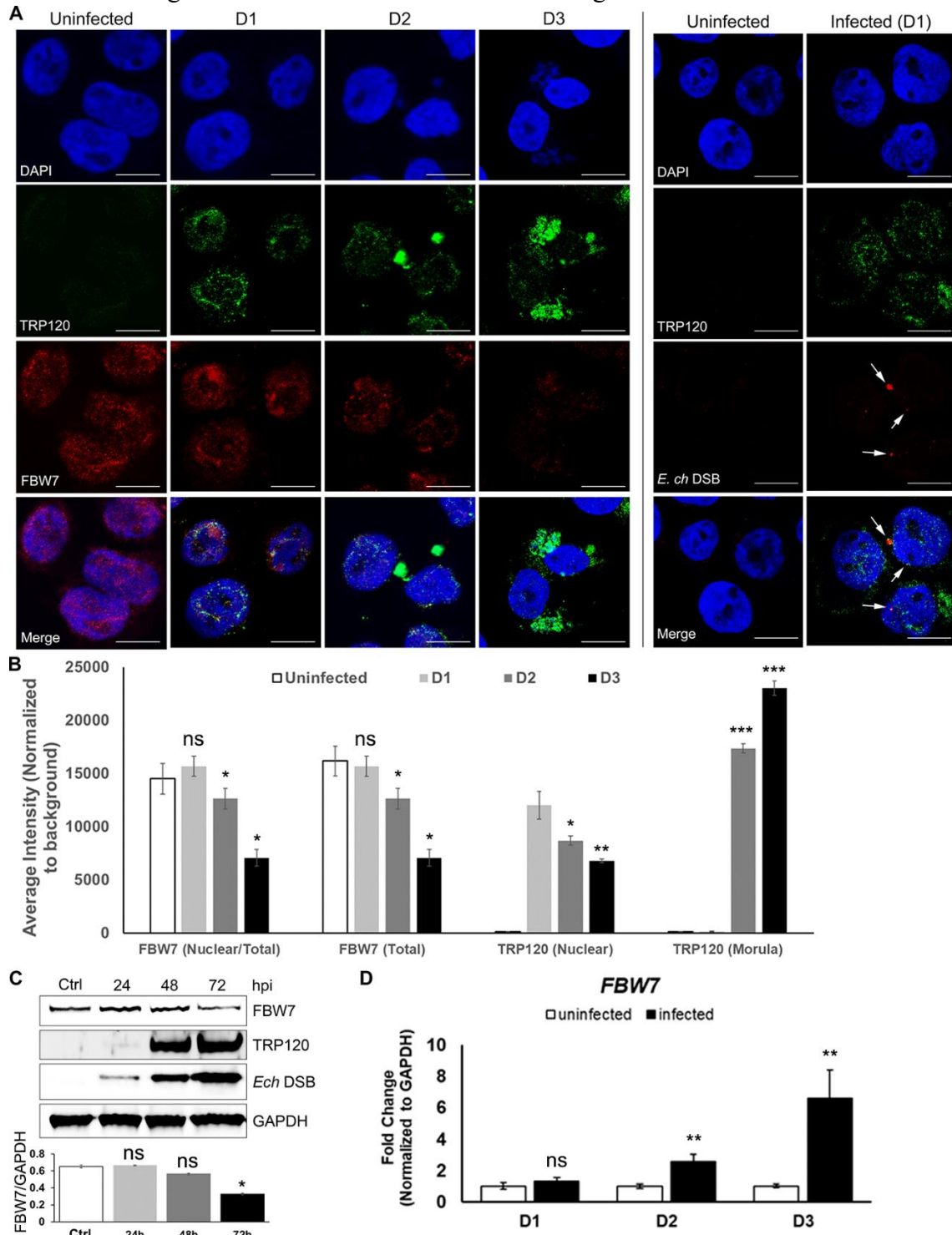
In vitro pull-down was performed to demonstrate direct interaction between recombinant *E. chaffeensis* TRP120 tandem-repeat (TR) domain protein with recombinant FBW7 FBOX and WD40 domains. cOmplete His-Tag purification resin was used to pull down FBOX-His and WD40-His proteins, and bound TRP120-TR-GST was detected with anti-GST and anti-TRP120 antibodies.

also illustrated strong colocalization intensity with Mander's coefficient values of 0.935 and 0.971, indicating majority of TRP120-GFP in the cell colocalized with either FBW7-FBOX or FBW7-WD40. Overall, these findings demonstrate that TRP120 colocalizes specifically with the FBOX and WD40 domains, but not the N-terminus of FBW7.

FBW7 is degraded during *E. chaffeensis* infection.

There are several mechanisms for cellular protein regulation, and FBW7 is a well characterized component of the SCF E3 Ub ligase that targets oncoproteins for degradation [31]. However, the molecular mechanisms of FBW7 regulation are not well understood. Recent evidence has shown that FBW7 has multiple upstream regulators such as p53, Pin1, C/EBP-d, Hes-5, Numb, parkin and several microRNAs [49-55]. In order to understand the mechanism of FBW7 regulation during infection, confocal immunofluorescent microscopy was performed on uninfected and *E. chaffeensis*-infected THP-1 cells on days 1, 2 and 3 post-infection (Fig. 3A). In uninfected THP-1 cells, FBW7 was observed in both nucleus and cytoplasm; however, by day 1 post-infection FBW7 was only observed in the nucleus with TRP120. *E. chaffeensis* Dsb staining confirmed *E. chaffeensis* infection of THP-1 cells at 24 hpi in which TRP120 was observed in the nucleus but was not detected on ehrlichial morulae. By 48 hpi, TRP120 was primarily observed colocalizing with the morulae but was still present in the nucleus colocalizing with significantly lower levels of FBW7. At 72 hpi, FBW7 nuclear presence was further reduced (>70%) compared to uninfected cells, while TRP120 nuclear level was also reduced (~40%) with significantly increased TRP120 presence on the morulae. The fluorescent intensities of FBW7 and TRP120 from the confocal microscopic images were quantified using image J (Fig. 3B), illustrating a temporal decrease in expressions of both nuclear FBW7 and TRP120 levels with significantly increased expression of TRP120 on maturing morulae. In addition, FBW7 levels were also quantified using Western immunoblot analysis of whole cell lysates extracted from infected THP-1 cells at 24, 48 and 72 hpi, with uninfected control cells harvested at the same given time points

(only a single time point was shown as significant differences were not observed among uninfected cells) (Fig. 3C). Consistent with FBW7 visualization by confocal microscopy, there was a gradual reduction in FBW7 levels throughout infection while overall TRP120



levels increased as the infection progressed. But more importantly, nuclear TRP120

Figure 3: FBW7 is degraded during *E. chaffeensis* infection.

A. Confocal immunofluorescent microscopy was performed to observe colocalization of TRP120 (green) with FBW7 (red) and the temporal changes in FBW7 levels during *E. chaffeensis* infection. DAPI was used for nuclear staining (blue). In uninfected cells, FBW7 was primarily observed in the nucleus but was also detectable in the cytoplasm. Day 1 post-infection (pi), FBW7 was detected only in the nucleus and colocalization with TRP120 was observed. By day 2 pi, FBW7 levels decreased ~50% and ~70%, respectively compared to uninfected controls. TRP120 levels decreased in nucleus and increased TRP120 was associated with the morulae 48 and 72 hpi. Confocal immunofluorescent microscopy confirming *E. chaffeensis* infection at day 1 pi (presented in the right panel separated by line) with cytoplasmic *E. chaffeensis* Dsb (red) detection, also demonstrated nuclear expression of TRP120 (green). For each time point, 3 fields of 30 cells were analyzed (n=30). **B.** FBW7 and TRP120 fluorescent intensities from the confocal immunofluorescent microscopy (A) were calculated using image J and graphically demonstrated significant nuclear reduction in FBW7 intensity (normalized to total fluorescent intensity) at D2 ($p<0.05$) and D3 pi ($p<0.05$) with presence of nuclear TRP120. A reduction of nuclear TRP120 was also observed at D2 ($p<0.05$) and D3 pi ($p<0.005$) compared to D1 pi, while there was a significant increase of TRP120 in the morulae ($p<0.0005$ for both time points). **C.** Western immunoblots of whole cell lysates harvested from THP-1 cells infected with cell-free *E. chaffeensis* for 24, 48 and 72 h with uninfected (ctrl) cells harvested at the same time points identified. Significant decrease of FBW7 level was detected by 72 hpi compared to ctrl ($p<0.05$). n=4. **D.** Quantitative RT-PCR analysis of *FBW7* expression was performed using cDNA from infected THP-1 cells at 24, 48 and 72 hpi shows a significant increase in *FBW7* expression during infection at 48 and 72 hpi compared to uninfected control ($p<0.005$). GAPDH was used as endogenous control. The analysis was performed from data collected from 3 experiments and technical replicates.

remained present throughout infection (Fig. 3A-B). These results demonstrate that ehrlichial infection and persistent nuclear TRP120 levels coincide with a decrease in FBW7. To investigate FBW7 regulation during *E. chaffeensis* infection and the molecular mechanisms involved, qRT-PCR was performed to assess temporal changes in *FBW7* mRNA expression. The results demonstrated progressively increased levels of *FBW7* expression 24, 48, and 72 hpi (Fig. 3D). The decrease in FBW7 protein levels as transcriptional upregulation occurs suggests that FBW7 is post-translationally regulated during infection.

FBW7 degradation results in increased levels of FBW7 regulated oncoproteins.

In certain cancers, degradation or loss of FBW7 function results in increased levels of FBW7 oncoprotein substrates [32]. Notch1 intracellular domain (NICD), c-Jun, MCL1 and cMYC are well characterized and important FBW7-regulated oncoproteins in which overexpression correlates with tumorigenesis [56]. These oncoproteins are also key

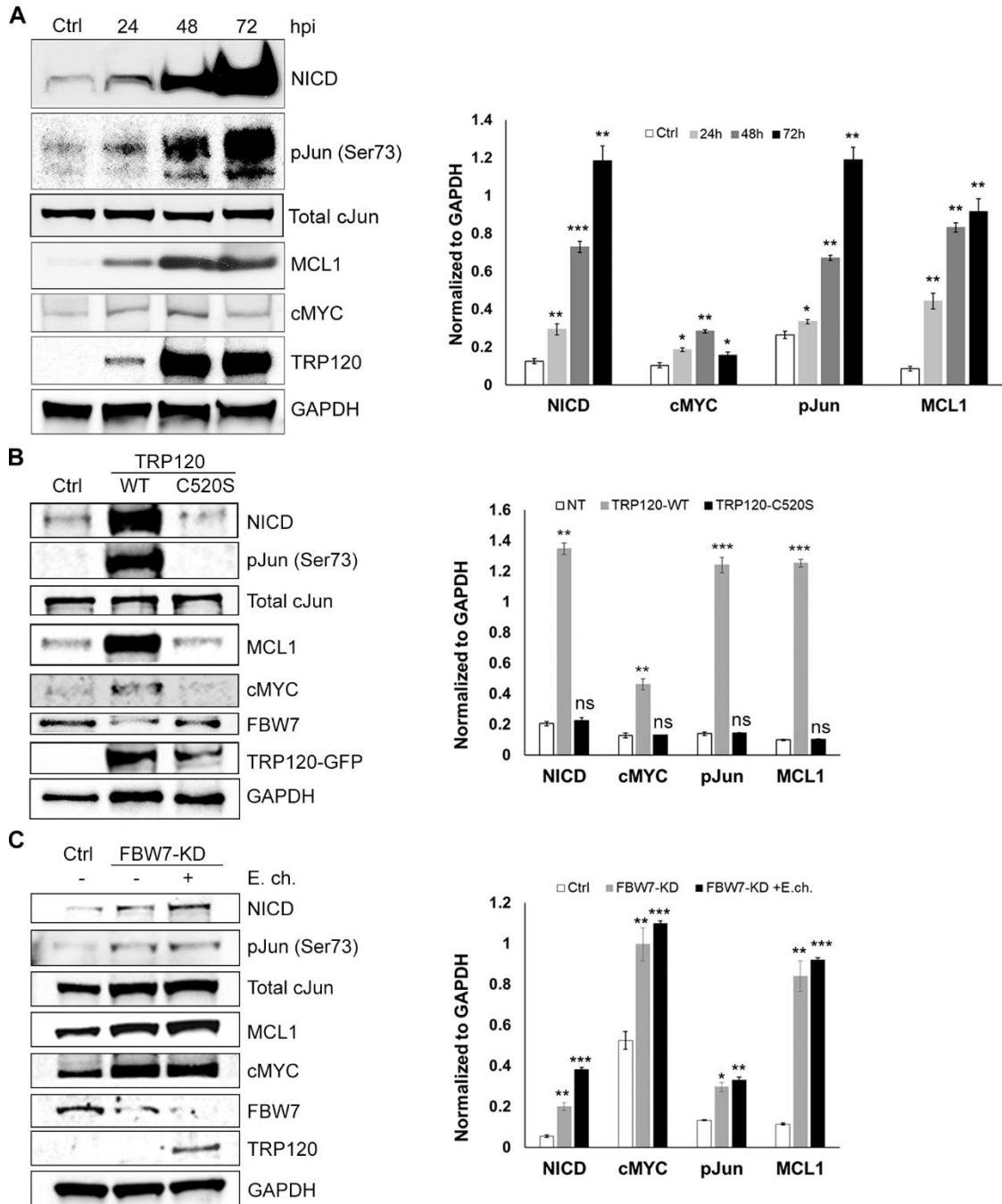


Figure 4: Levels of FBW7-regulated oncoproteins are increased during *E. chaffeensis* infection.

A. Western immunoblots demonstrating stabilization and upregulation of FBW7 downstream targets: Notch1 intracellular domain (NICD), cMYC, phospho-Jun (p-Jun) and MCL1. Western immunoblots of NICD, cMYC, p-Jun, total c-Jun and MCL1 levels 24, 48 and 72 hpi. GAPDH was used as loading control, and TRP120 to confirm *E. chaffeensis* infection (n=3). Significant temporal increases in NICD, cMYC, p-Jun and MCL1 levels were observed during *E. chaffeensis* infection. Densitometry of Western immunoblots (A) was performed to determine levels of each protein using Image J comparing each infected time point to uninfected. Phospho-Jun was additionally normalized to the levels of total c-Jun, then normalized again to the levels of GAPDH (* $p < 0.05$, ** $p < 0.005$, and *** $p < 0.0005$). **B.** Western immunoblots of uninfected HeLa cells transfected with catalytic-inactive TRP120 (TRP120-C520S) to demonstrate protein levels of NICD, phospho-Jun, MCL1 and cMYC. Densitometry values were measured in ImageJ and plotted (right) to determine the levels of oncoprotein in uninfected cells transfected with TRP120-C520S to be statistically insignificant (ns) compared to control cells (n=3). **C.** Western immunoblots demonstrating significant increase of protein levels of NICD, p-Jun, MCL1 and cMYC in both uninfected and infected THP-1 cells with FBW7-KD, compared to uninfected, scrambled siRNA controls (n=3). Densitometry values were measured in ImageJ and plotted (right), and statistical analysis was calculated for oncoprotein levels in siFBW7 treated cells compared to control (* $p < 0.05$, ** $p < 0.005$, and *** $p < 0.0005$).

regulators of cell proliferation, differentiation, and apoptosis [57-59]. Recently, we reported that the Notch signaling pathway is activated during *E. chaffeensis* infection by TRP120, resulting in downregulation of TLR2/4 expression [26]. Here we also observed a significant increase in NICD protein levels (Fig. 4A). Activation of the Notch signaling pathway is important in ehrlichial survival and elevated protein levels of NICD suggest that infected cells maintain constitutive pathway activation during infection. Moreover, levels of cellular apoptosis inhibitors phosphorylated c-Jun (p-c-Jun) and MCL1 were also significantly elevated (Fig. 4A). Interestingly, cMYC levels progressively increased at 24 and 48 hpi, but were significantly reduced at 72 hpi (Fig. 4A). Furthermore, when uninfected cells were transfected with catalytic-inactive TRP120 (TRP120-C520S), resulting in retention of FBW7 function, these oncoproteins remained at a similar level to

control cells (Fig. 4B). In addition, oncoprotein levels were examined in both FBW7-KD and FBW7-KD with 24 hpi cells, where the levels were significantly increased compared to uninfected, scrambled siRNA-transfected control (Fig. 4C). These results further suggest that TRP120-mediated degradation of FBW7 significantly increased the levels of p-c-Jun, MCL1 and cMYC in order to repress host cell apoptosis.

FBW7 degradation during infection is K48-Ub-dependent.

While post-translational regulation of FBW7 is not well studied, there is evidence demonstrating that autoubiquitination is the primary mechanism for self-regulation and turnover [60]. In the absence of downstream substrates, FBW7 is ubiquitinated within the SCF complex by an autocatalytic reaction, which leads to its proteasomal degradation [61]. Other studies have also reported that in neurons, parkin promotes FBW7 β ubiquitination-dependent degradation; however, the exact mechanism was not determined [52]. For a protein to be targeted by the 26S proteasome, it must be ubiquitinated with a polyubiquitin chain such as K48-Ub. To determine whether FBW7 was ubiquitinated with K48-Ub, co-IP was performed to examine the ubiquitination status of FBW7 during ehrlichial infection (Fig. 5A). FBW7 was immunoprecipitated from *E. chaffeensis*-infected and uninfected cells harvested at 0, 24 and 48 hpi and treated with NEM and Bortezomib to inhibit deubiquitination and degradation. The immunoblots revealed a constitutive level of ubiquitinated FBW7 (Ub-FBW7, 200 kDa) in uninfected control cells, which is consistent with maintenance of FBW7 levels by K48 autoubiquitination. In infected cells, K48-ubiquitinated FBW7 levels increased in bortezomib-treated cells. Moreover, decreased FBW7 was observed at 24, 48 and 72 hpi in untreated cells, but was stable throughout infection in bortezomib-treated (10ng/ml, 10 h) cells (Fig. 5B-C).

These results further suggest that increased FBW7 degradation during *E. chaffeensis*

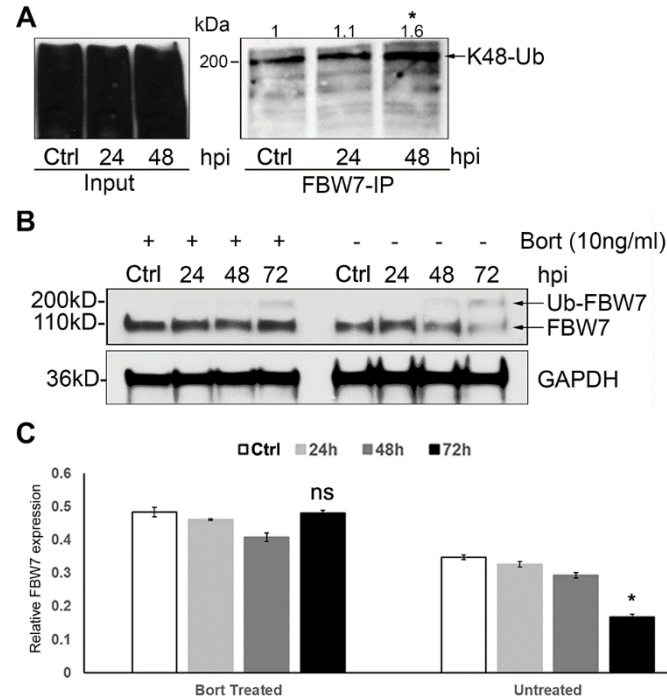


Figure 5: FBW7 is ubiquitinated with K48-Ub and degraded by the proteasome.

A. Immunoprecipitation of K48-Ub FBW7 from uninfected and *E. chaffeensis*-infected THP-1 cells demonstrating increased levels of FBW7 K48-Ub. Lysates were treated with NEM (*N*-ethylmaleimide, equal mass amount to whole cell lysates used) and Bortezomib (10ng/ml, 10 h) to prevent deubiquitination and proteasome degradation. Anti-K48-Ub antibody was used to pull down all K48-Ub conjugated proteins. Basal levels of K48-Ub FBW7 at ~200 kDa are observed indicating FBW7 undergoes K48-Ub as a mechanism of protein regulation and turnover. Densitometry values of K48-Ub-FBW7 bands were denoted on top of each band for every time point, and a $p < 0.05$ significance comparing 48 hpi to uninfected control (0 hpi) was calculated from three experiments ($n = 3$). **B.** Western immunoblots demonstrating the effect of Bortezomib (Bort, 26S proteasome inhibitor) on FBW7 during infection. Whole cell lysates were obtained from both Bort-treated (10ng/ml, 10 h) and untreated groups infected with cell-free *E. chaffeensis* and uninfected controls at 24, 48 and 72 hpi. Uninfected cells were harvested at the same time points (24, 48 and 72 hpi) with only a single time point (ctrl) shown in the figure as significant differences were not observed among uninfected cells. FBW7 levels remained unchanged during infection in the Bort treated group; however, there was a temporal reduction of FBW7 levels in untreated group, demonstrating FBW7 proteasomal degradation during infection. **C.** Densitometry of Western immunoblots (B) performed using image J. Statistical analysis was done by comparing data from infected cells to control cells at respective time points ($n = 3$). A $p < 0.05$ significance was determined for FBW7 level at 72 hpi in the untreated group compared to uninfected control in the same group.

infection occurs through K48 ubiquitination and is proteasome-dependent.

TRP120 ubiquitinates FBW7 for degradation.

TRP120 has HECT E3 ligase activity and one host cell substrate (PCGF5) has been identified [29]. Thus, we considered that FBW7 could be another TRP120 substrate. To examine this question, we transfected TRP120-GFP in HeLa cells to determine if ectopically expressed TRP120 affected FBW7 stability. Indeed, when HeLa cells were transfected with TRP120-GFP plasmid for 24 and 48 h, there was a progressive reduction

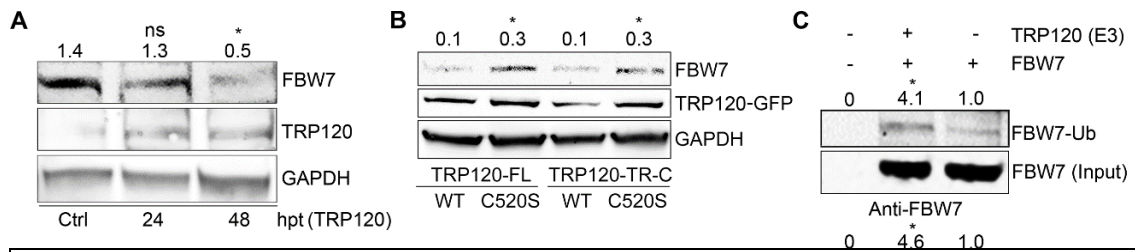


Figure 6: *E. chaffeensis* TRP120 HECT E3 Ub ligase activity mediates K48 ubiquitination and degradation of FBW7.

A. Levels of FBW7 decrease in HeLa cells ectopically expressing TRP120-GFP at 0, 24, and 48 hours post-transfection (hpt). Densitometry values of FBW7 for each time point were denoted above respective bands (ctrl: 1.4 ± 0.03 ; 24 hpt: 1.3 ± 0.08 ; 48 hpt: 0.5 ± 0.09), with Significantly ($p < 0.05$) decreased levels of FBW7 were detected at 48 hpt with TRP120 compared to control ($n = 3$). **B.** HeLa cells were transfected with TRP120 WT and HECT E3 ligase catalytic mutants (TRP120-FL-C520S and TRP120-TR-C-C520S). Increased degradation of endogenous FBW7 was detected in TRP120-WT compared TRP120-C520S mutants lacking Ub ligase function. Densitometry values of FBW7 for each sample group were labeled above respective bands (TRP120-FL-WT: 0.1 ± 0.02 ; TRP120-FL-C520S: 0.3 ± 0.04 ; TRP120-TR-C-WT: 0.1 ± 0.004 ; TRP120-TR-C-C520S: 0.3 ± 0.03), with $p < 0.05$ significance for both TRP120 transfection groups (TRP120-FL and TRP120-TR-C) comparing levels of FBW7 in cells transfected with catalytic-inactive TRP120 mutant (C520S) to wildtype TRP120 (WT) ($n = 3$). **C.** *In vitro* ubiquitination of native FBW7 by *E. chaffeensis* rTRP120 using anti-FBW7 and anti-K48 antibodies for detection. Increased FBW-Ub was detected at ~200 kDa in the presence of rTRP120 compared to controls without TRP120. K48 Ub was also detected on FBW7-Ub in the presence of rTRP120 indicating TRP120 directly ubiquitinates FBW7 with K48-Ub chains. Densitometry values of both FBW7-Ub (FBW7+TRP120: 4.1 ± 0.17 ; FBW7-TRP120: 1.0 ± 0.02) and K48-Ub (FBW7+TRP120: 4.6 ± 0.06 ; FBW7-TRP120: 1.0 ± 0.01) were denoted above each bands, with $p < 0.05$ significance comparing levels of either FBW7-Ub or K48-Ub in the presence of rTRP120 to the absence of rTRP120 as E3 ligase ($n = 4$).

of FBW7 level from 0-48 h post-transfection compared with controls (Fig. 6A). These results indicate that TRP120 does impact FBW7 stability. We then compared FBW7 stability in HeLa cells transfected with TRP120-WT and TRP120-C520S, a mutant TRP120 lacking the E3 ligase function. FBW7 stability was increased in cells expressing TRP120-C520S compared to TRP120-WT. In addition, cells expressing TRP120-TR-C-C520S, a truncated TRP120 containing only the TR domains and mutant C-terminus, also resulted in stability of FBW7 further demonstrating FBW7 is a TRP120 substrate (Fig 6B). To confirm that FBW7 is a TRP120 substrate, *in vitro* ubiquitination assays were performed to demonstrate TRP120 directly ubiquitinates FBW7. The *in vitro* ubiquitination experiment revealed that in the presence of rTRP120, Ub-FBW7 (~200 kDa) was detected at higher levels compared controls. Similarly, increased K48-Ub was detected on FBW7 in the presence of rTRP120 (Fig 6C), which indicates that TRP120 ubiquitinates FBW7 with K48-Ub for degradation. Furthermore, the elimination of TRP120 N-terminus did not affect TRP120 Ub ligase activity in the degradation of FBW7 demonstrating that the TRP120 N-terminal domain has no role in the interaction or in TRP120 Ub ligase activity. Collectively, these results demonstrate that FBW7 is a substrate of TRP120 Ub ligase activity, resulting in FBW7 proteasomal degradation.

Changes in FBW7 levels impact *E. chaffeensis* infection.

We examined the effect of FBW7 on *E. chaffeensis* infection using siRNA knockdown of FBW7 in THP-1 cells. *E. chaffeensis* infection was significantly and progressively increased by 50% by 48 hpi in FBW7-KD cells compared to control transfected with scrambled siRNA (Fig. 7A). Conversely, when FBW7 was overexpressed in infected HeLa cells, *E. chaffeensis* infection was reduced up to 3-fold compared to infected control cells (Fig. 7B). Collectively, these results further support the conclusion that FBW7 stability plays a crucial role in promoting *E. chaffeensis* intracellular survival and infection in monocytes.

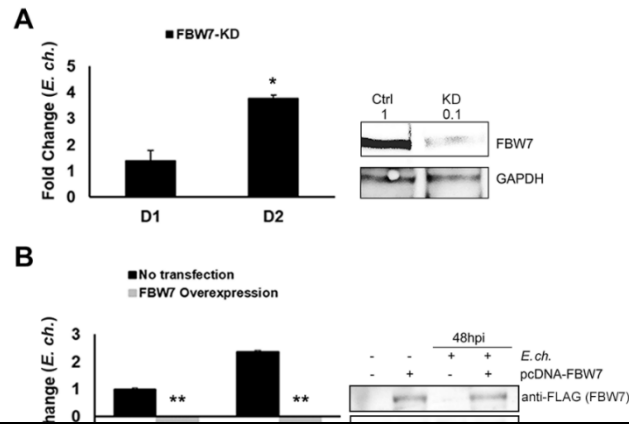


Figure 7: Changes in FBW7 levels impact *E. chaffeensis* infection.

A. iRNA knockdown of FBW7 in *E. chaffeensis*-infected THP-1 cells at 24 and 48 hpi. Scrambled siRNA was used as RNAi control. Western immunoblot (right) demonstrated ~90% knockdown (KD) of FBW7, densitometry values were labeled above each band. Cells were harvested for qPCR to assess changes in *E. chaffeensis* infection. For all the data points from both uninfected and infected KD cells, the data was first normalized to cells transfected scrambled siRNA (infected and uninfected, respectively). Then, the infected group was normalized to uninfected group to determine the fold change. A significant increase (3-fold) in *E. chaffeensis* load was detected in FBW7-KD cells ($p \leq 0.05$). **B.** Overexpression of FBW7 was achieved by transfecting HeLa cells with pcDNA3.1+/C-(K) DYK-FBW7 (denoted as pcDNA-FBW7 in the figure), and negatively impacted *E. chaffeensis* infection ($p \leq 0.005$) in infected HeLa cells. Quantitative PCR analysis was performed similarly to panel A. Western Immunoblot (right) confirmed ectopic overexpression of FBW7. For both panels A and B, the data shown is representative of 3 experiments (n=3) with technical replicates (n=3).

DISCUSSION

Recent investigations of *E. chaffeensis* pathobiology have revealed how TRP effectors exploit host signaling and post translational pathways and other cellular processes in order to evade host innate immune mechanisms and establish intracellular infection [21, 36, 62-64]. Specifically, *E. chaffeensis* has evolved mechanisms to avoid recognition by innate immune receptors and destruction in the phagolysosome, inhibit apoptosis, and alter cellular signaling required for host cell defense function [65].

Recently, we reported that *E. chaffeensis* exploits evolutionarily conserved host cell signaling pathways such as Wnt and Notch to modulate innate host defenses to promote infection in monocytes [24, 26]. Both Wnt and Notch are known for their role in regulating cellular proliferation and cell fate, but they have also been shown to influence innate immune defenses such as apoptosis and autophagy [66, 67], and previous studies have determined the Notch signaling regulates TLR expression [68, 69]. Notably, we have recently determined that *E. chaffeensis* exploitation of Notch signaling downregulates TLR2/4 expression during infection [26].

In a previous study, we reported that FBW7, a negative regulator of Notch, interacted with TRP120 [22]. Three FBW7 isoforms with similar function occupy distinct subcellular compartments. With regards to the present investigation, FBW7 α (referred as FBW7 in this study) is the most abundantly expressed and is found in the nucleus of many cell types, including monocytes. It is primarily found in the nucleus due to the presence of two canonical NLS sequence motifs where it functions as the substrate recognition subunit of the SCF E3 ligase complex [38,40,168]. Studies have shown that FBW7 negatively regulates downstream substrates strictly in the nucleus through K48

ubiquitination to facilitate proteasomal degradation [55,169-172]. However, when FBW7 is displaced from the nucleus through deletion of the NLS sequence motifs, the SCF complex becomes unstable and unable to ubiquitinate downstream substrates [173,174].

TRP120 has been shown to translocate to the host cell nucleus where it binds host genes associated with transcriptional regulation, signal transduction and apoptosis [22]. Thus, we explored the molecular details of the interaction between *E. chaffeensis* TRP120 and FBW7 in the host cell nucleus and determined the fate and regulatory mechanism of FBW7 as a result of this interaction. Strong colocalization was observed with confocal microscopy between TRP120 and FBW7 primarily in the nucleus at early time points during infection, which is consistent with the temporal/spatial dynamics of TRP120 nuclear translocation and function. Furthermore, ectopic expression results revealed that TRP120 colocalizes with adjacent FBOX and WD40 domains of FBW7, suggesting the interaction with these domains may facilitate ubiquitination of lysine residues within FBW7.

Under normal cellular conditions, FBW7 regulation occurs at both transcriptional and post-translational levels [61]. Transcriptional regulation of FBW7 includes CCAAT/enhancer-binding protein delta (CEPB δ), and it has been shown to directly inhibit FBW7 expression; Hes5, a downstream target of Notch signaling, has also been reported to repress FBW7 expression [54, 70-72]. Other studies have reported that miRNA-27a, miRNA-223 and miRNA-25 inhibit the expression of FBW7 to promote tumorigenesis [73-76]. However, the main mechanism involved in FBW7 turnover appears to be autoubiquitination [60]. In the absence of substrates, autoubiquitination of FBW7 occurs within the SCF complex, and is dependent on phosphorylation priming at

Ser227 then facilitated by the peptidyl-prolyl cis/trans isomerase Pin1 [49]. Another study demonstrates E3 ligase parkin ubiquitinates FBW7 β in the neurons; however, the exact molecular mechanism is not known [52]. In the context of *E. chaffeensis* infection of monocytes, we have determined that FBW7 is progressively degraded and the level of FBW7 is not restored at any time during infection despite upregulated *FBW7* gene expression. Further investigation demonstrated that the decrease in FBW7 is independent of transcriptional regulation. Instead, FBW7 levels begin to decrease after TRP120 translocation into the nucleus and progressively decrease during infection. This finding suggests that TRP120 negatively regulates FBW7 in order to stabilize downstream oncoproteins involved in regulation of cell proliferation and survival, thereby impacting *E. chaffeensis* infection.

E. chaffeensis survival is dependent on activation of cell signaling pathways, such as Wnt and Notch to regulate cellular proliferation, differentiation and innate host defenses including autophagy and apoptosis [66]. Despite the well characterized role of the Notch pathway in cell differentiation, less is known regarding its role in regulating innate immunity. However, accumulating evidence has shown a complex role of Notch signaling pathway in innate immunity regulation [68, 69, 77]. During *E. chaffeensis* infection, we have determined that TRP120 not only acts as nucleomodulin to upregulate *NOTCH1* transcription but is also functions as Notch ligand mimic to activate Notch signaling [21, 24, 26]. Moreover, as demonstrated in this investigation, TRP120 E3 ligase activity is involved in regulating Notch signaling by degrading the negative regulator FBW7 to maintain Notch signaling. These findings not only reveal the importance of Notch signaling pathway in promoting infection, but also highlight the unique

moonlighting functions of TRP120. Notably, this is the first bacterial effector shown to exhibit such a diversity of functions in different cellular contexts during infection including direct activation and regulation of the same signaling pathway.

The TRP120-FBW7 interaction results in stabilization of other well-known oncoproteins. As occurs in tumor cells, the reduction of FBW7 leads to increased levels of anti-apoptotic proteins p-c-Jun, MCL1 and cMYC during ehrlichial infection. Oncoprotein c-Jun is part of the JNK signaling pathway that plays a vital role in apoptosis, inflammation, cytokine production and metabolism [78]. Through a series of phosphorylation events, c-Jun is phosphorylated and activated for downstream AP-1 gene transcription that contributes to diverse regulatory mechanisms involved in cell proliferation, cell differentiation and apoptosis [79]. However, like in tumor cells, elevated transcription factor p-c-Jun is observed as a response to the degradation of FBW7, and we have also shown direct *E. chaffeensis* TRP32 nucleomodulin-mediated upregulation of *JUN* expression during infection [80]. Like Notch, both upregulation of mRNA expression and elevation of protein levels suggests that the stabilization of c-Jun activity is crucial for *E. chaffeensis* intracellular survival. This is also complemented by the increase in MCL1 protein levels, an anti-apoptotic member of the BCL-2 family known to block the release of cytochrome *c* that signals for cell death [81, 82]. Although the oncoproteins regulated by FBW7 increased, cMYC does not exhibit the same temporal levels we noted with NICD, p-c-Jun and MCL1. Instead, the decrease in cMYC level at 72 hpi correlates with the downregulation in *MYC* expression reported during infection. The proportional reduction in *MYC* expression suggests a negative feedback mechanism to modulate cMYC levels in the cells that eventually overwhelms the

accumulation of cMYC from the loss of FBW7 [24, 84]. Finally, we have revealed that TRP120-FBW7 interaction regulates downstream oncoproteins NICD, cMYC, c-Jun and MCL1, which appear to play essential roles in delaying host cell apoptosis, and further studies are required to fully understand their roles in promoting *E. chaffeensis* infection.

Several bacterial effectors are known to target host proteins to manipulate the host ubiquitination system, such as *Shigella* OspI and OspG which interact with host E2 proteins. In addition, *Salmonella* SopA has HECT E3 ligase activity that has been suggested to play a regulatory role in host ubiquitination pathways [84-88]. A recent study reported that *Salmonella* SopA enhances ubiquitination of host protein TRIM65 to modulate innate immune responses by inducing interferon- β expression [89]. However, other specific host substrates that interact with OspI, OspG or SopA have not been identified. Notably, a TRP120 HECT ligase substrate (PCGF5) has been identified [29]. The interaction between TRP120 and PCGF5 has been shown to occur in the nucleus during early infection (24 h) and with cytoplasmic morulae during late infection (72 h) [36]; however, TRP120 appears to interact with FBW7 in the nucleus throughout the course of infection resulting in Ub-mediated degradation of FBW7.

We have previously demonstrated TRP120 Ub ligase function and identified PCGFs as host substrates. This study identifies another TRP120 Ub ligase substrate and further demonstrates the role of TRP120 in regulating the levels of specific host cell proteins that are known to interact with TRP120. We demonstrated that TRP120 targets FBW7 with K48-Ub linkage chain, which is one of the major post translational modification events leading to proteasomal degradation [90]. In addition, K48 ubiquitination of FBW7 occurs through the functional TR and C-terminal domains of TRP120 and does not require the

N-terminus. This is consistent with previous reports that have demonstrated the TR domain of TRP120 is important for interactions with host cell proteins, and the C-terminal domain has conserved HECT ligase catalytic domain [14, 22, 29]. Notably, a major finding of this investigation is the identification of FBW7 as the second TRP120 E3 ligase substrate, and *E. chaffeensis* is the only pathogen to our knowledge that targets FBW7 during infection.

The TRP120-FBW7 interaction reveals that the TRP120-mediated ubiquitination-dependent degradation of FBW7 is critical for *E. chaffeensis* infection. We have previously shown that the reductions in FBW7 through iRNA knockdown leads to enhanced ehrlichial infection [33]. In this study, we have determined that degradation of FBW7 by TRP120 E3 ligase activity is a mechanism to reduce FBW7 levels. In addition, reintroduction of FBW7 most likely inhibits downstream pro-survival NICD, c-Jun,

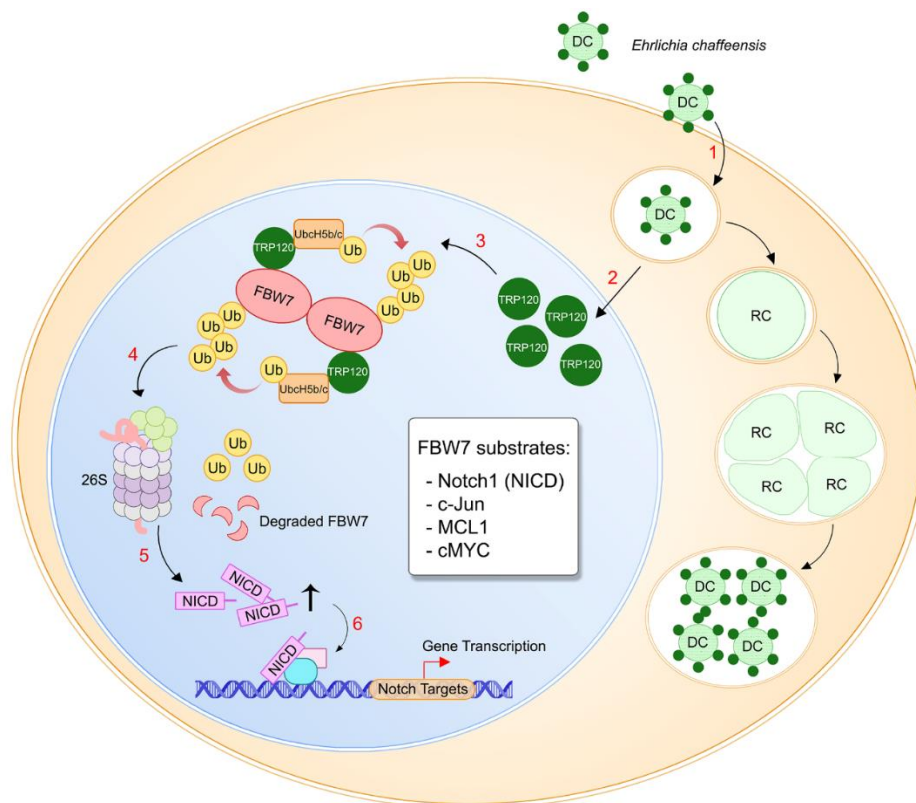


Figure 8: Proposed model of *E. chaffeensis* TRP120 HECT E3 ligase regulation of FBW7 during infection.

(1) Infectious dense-cored *E. chaffeensis* expressing TRP120 on the surface enter host monocytes through receptor-mediated phagocytosis and replicate in a cytoplasmic vacuole that does not fuse with lysosomes; (2) TRP120 is secreted via type-1 secretion system into host cell within 3 h of entry and translocates into the host nucleus; (3) TRP120 binds to phosphorylated FBW7 homodimer in trans conformation and ubiquitinates with K48-Ub chains; (4) FBW7-K48-Ub is then degraded by the 26S proteasome, presumably in the nucleus; (5) TRP120-mediated degradation of FBW7 leads to stabilization and accumulation of downstream oncoprotein targets including NICD, c-Jun, MCL1 and cMYC; (6) Pro-survival oncoproteins activate downstream gene transcription to delay host cell apoptosis to promote *E. chaffeensis* infection.

MCL1 and possibly cMYC cell signaling to restore monocyte apoptosis, thus preventing cell survival and propagation of *E. chaffeensis* infection. This strongly supports the importance of TRP120-mediated degradation of FBW7 in the maintenance of Notch signaling as a mechanism to prevent apoptosis to promote *E. chaffeensis* infection.

Through this investigation, we have gained an understanding of the importance of TRP120 interaction with FBW7 during *E. chaffeensis* infection. An overview of this interaction and downstream effects are illustrated by the proposed model (Fig. 8) that can be summarized as follows: 1) *E. chaffeensis* attaches and enters a monocyte as dense-core ehrlichia where TRP120 is expressed on the bacterial surface; 2) TRP120 is secreted via type-1 secretion system, and translocates to the host cell nucleus via an unknown mechanism; 3) TRP120 ubiquitinates FBW7 in the nucleus; 4) K48-Ub-FBW7 is then degraded by the 26S proteasome most likely in the nucleus; 5) degradation of FBW7 results in increased levels of downstream pro-survival markers (NICD, p-c-Jun, MCL1 and cMYC) resulting in the maintenance of Notch signaling activation and anti-apoptotic programming; 6) finally, the pro-survival markers activate downstream gene expression

to suppress host innate immunity and delay monocyte apoptosis, thus creating a favorable environment for *E. chaffeensis* replication.

Chapter 4. Summary and Future Directions

This project was proposed to study the interaction between *Ehrlichia chaffeensis* effector TRP120 and host tumor suppressor FBW7. In this work, I was successful at completing the aims set out to provide support for the hypothesis that TRP120 ubiquitinates FBW7 for degradation and results in the maintenance and amplification of Notch signaling and other downstream pro-survival proteins to promote infection.

In Chapter 3, I first showed through confocal microscopy that TRP120 indeed translocates into the host nucleus during early infection to interact with FBW7, more specifically I identified that TRP120 interacts with the FBOX and WD40 domains of FBW7, which binds to the SKP1 of the E3 ligase complex and downstream substrates, respectively. The binding of TRP120 at these domains is interesting and provides insight to how TRP120 is regulating FBW7. In fact, through Western blot analyses, I found that the protein levels of FBW7 are decreased over the course of infection and treatment with bortezomib retains the levels of FBW7, and this event is independent of transcriptional regulation. These results are further evidence that FBW7 is degraded during infection.

Secondly, I observed nuclear colocalization of TRP120 with FBW7 throughout the course of infection. Moreover, this interaction leads to degradation of FBW7, which is predominantly expressed in the host nucleus. This observation suggests the TRP120-FBW7 interaction can be described as part of TRP120 nucleomodulin activity. With additional experiments, I demonstrated TRP120 ubiquitinates FBW7 with K48-Ub linkage chains that results in the degradation of the tumor suppressor. This provides increasing support for my hypothesis that FBW7 is a substrate of TRP120 ubiquitin ligase activity, and it also provides further support that TRP120 moonlights as ubiquitin

ligase as another characterization of its many nucleomodulin functions. Hopefully, future studies will lead to identification of additional host substrates that will strengthen this observation.

In addition, I showed that the downstream oncoproteins targets of FBW7, Notch, c-Jun, MCL1 and cMYC, are stabilized during infection. Unlike Notch, c-Jun and MCL1, the levels of cMYC begin to decrease at around 72 hpi, suggesting other factors may be playing a role in regulating cMYC. A topic for future research could address the role of cMYC during ehrlichial infection and identify any possible ehrlichial effectors that might be involved in regulation of this protein. Nevertheless, Notch, c-Jun and MCL1 levels are significantly increased during infection, suggesting that upregulation of these proteins is important in maintaining intracellular survival and promoting infection, possibly by stabilizing the anti-apoptotic function of these proteins. Furthermore, ectopic expression of WT TRP120 leads to degradation of FBW7 and results in increased levels of Notch, c-Jun, MCL1 and cMYC, while catalytic inactive mutant TRP120 (TRP120-C520S) expression does not result in stabilization of these oncoproteins. These results further support that the loss of FBW7 is TRP120 mediated and ubiquitination-dependent, and such loss of negative regulatory function leads to stabilization of these downstream oncoproteins, which are also anti-apoptotic. However, gene expression of downstream targets for these anti-apoptotic proteins during ehrlichial infection is currently unknown. Future studies will determine the roles of Notch, c-Jun and MCL1 in delaying or preventing host cell apoptosis as a mechanism for *E. chaffeensis* to promote infection.

Finally, I confirmed that siRNA knockdown of *FBW7* results in increased ehrlichial infection, and showed that overexpression of *FBW7* negatively impacts infection. The

results provide increasing support that the loss of FBW7 is essential for ehrlichial infection and the role of TRP120 as ubiquitin ligase is crucial for survival. Of course, among the ~100 host binding partners of TRP120, FBW7 is not the only protein that plays an important part. Future studies will continue to discover more integral players for *E. chaffeensis* intracellular survival and infection.

In summary, this project explored an important interaction between *E. chaffeensis* effector TRP120 and host binding partner FBW7, further elucidating the ubiquitin ligase function of a bacterial effector and the role it plays in promoting infection. And for the first time, it demonstrated the tumor suppressor FBW7 is targeted for degradation in the context of infection by an intracellular pathogen. This investigation additionally expanded our knowledge of TRP120 as a nucleomodulin that not only acts as a eukaryotic transcriptional regulator, but also utilizes ubiquitination to regulate host signaling pathways.

References

1. Cabezas-Cruz A, Zweggarth E, Vancová M, Broniszewska M, Grubhoffer L, Passos LMF, et al. *Ehrlichia minasensis* sp. nov., isolated from the tick *Rhipicephalus microplus*. *International journal of systematic and evolutionary microbiology*. 2016;66(3):1426-30. doi: doi:10.1099/ijsem.0.000895.
2. Cowdry EV. Studies on the Etiology of Heartwater: I. Observation of a Rickettsia, *Rickettsia ruminantium* (N. Sp.), in the Tissues of Infected Animals. *The Journal of experimental medicine*. 1925;42(2):231-52. PubMed PMID: 19869049; PubMed Central PMCID: PMCPMC2130998.
3. Rikihisa Y. The tribe Ehrlichieae and ehrlichial diseases. *ClinMicrobiolRev*. 1991; 4:286-308.
4. Anderson BE, Dawson JE, Jones DC, Wilson KH. *Ehrlichia chaffeensis*, a new species associated with human ehrlichiosis. *JClinMicrobiol*. 1991;29(12):2838-42.
5. Dumler JS, Barbet AF, Bekker CP, Dasch GA, Palmer GH, Ray SC, et al. Reorganization of genera in the families Rickettsiaceae and Anaplasmataceae in the order Rickettsiales: unification of some species of *Ehrlichia* with *Anaplasma*, *Cowdria* with *Ehrlichia* and *Ehrlichia* with *Neorickettsia*, descriptions of six new species combinations and designation of *Ehrlichia equi* and 'HGE agent' as subjective synonyms of *Ehrlichia phagocytophila*. *International journal of systematic and evolutionary microbiology*. 2001;51(Pt 6):2145-65. PubMed PMID: 11760958.
6. Maeda K, Markowitz N, Hawley RC, Ristic M, Cox D, McDade JE. Human infection with *Ehrlichia canis*, a leukocytic rickettsia. *NEnglJMed*. 1987;316:853-6.
7. Kawahara M, Ito T, Suto C, Shibata S, Rikihisa Y, Hata K, et al. Comparison of *Ehrlichia muris* strains isolated from wild mice and ticks and serologic survey of humans and animals with *E. muris* as antigen. *J Clin Microbiol*. 1999;37(4):1123-9.
8. Allsopp MTEP, Louw M, Meyer EC. *Ehrlichia ruminantium* – an emerging human pathogen. *S Afr Med J*. 2005;95.
9. Perez M, Bodor M, Zhang C, Xiong Q, Rikihisa Y. Human infection with *Ehrlichia canis* accompanied by clinical signs in Venezuela. *AnnNYAcadSci*. 2006;1078:110-7.
10. Pritt BS, Sloan LM, Johnson DK, Munderloh UG, Paskewitz SM, McElroy KM, et al. Emergence of a new pathogenic *Ehrlichia* species, Wisconsin and Minnesota, 2009. *NEnglJMed*. 2011;365(5):422-9.
11. Zhang, J., V. L. Popov, S. Gao, D. H. Walker, & X. Yu. (2007). The developmental cycle of *Ehrlichia chaffeensis* in vertebrate cells. *Cellular Microbiology*, 9(3), 610–618.
12. Mohan Kumar D, Yamaguchi M, Miura K, Lin M, Los M, Coy JF, et al. *Ehrlichia chaffeensis* Uses Its Surface Protein EtpE to Bind GPI-Anchored Protein DNase X

- and Trigger Entry into Mammalian Cells. *PLoS pathogens*. 2013;9(10):e1003666. doi: 10.1371/journal.ppat.1003666. PubMed PMID: 24098122; PubMed Central PMCID: PMC3789761.
13. Popov VL, Yu X, Walker DH. The 120 kDa outer membrane protein of *Ehrlichia chaffeensis*: preferential expression on dense-core cells and gene expression in *Escherichia coli* associated with attachment and entry. *Microb Pathog*. 2000;28(2):71-80. doi: 10.1006/mpat.1999.0327. PubMed PMID: 10644493.
 14. Wakeel, A., Kuriakose, J. A., & McBride, J. W. (2009). An *Ehrlichia chaffeensis* tandem repeat protein interacts with multiple host targets involved in cell signaling, transcriptional regulation, and vesicle trafficking. *Infection and Immunity*, 77, 1734-1745.
 15. Liu H, Bao W, Lin M, Niu H, Rikihisa Y. *Ehrlichia* type IV secretion effector ECH0825 is translocated to mitochondria and curbs ROS and apoptosis by upregulating host MnSOD. *Cellular microbiology*. 2012;14(7):1037-50. doi: 10.1111/j.1462-5822.2012.01775.x. PubMed PMID: 22348527; PubMed Central PMCID: PMC3371182.
 16. Lina TT, Farris T, Luo T, Mitra S, Zhu B, McBride JW. Hacker within! *Ehrlichia chaffeensis* Effector Driven Phagocyte Reprogramming Strategy. *Frontiers in cellular and infection microbiology*. 2016;6. doi: ARTN 5810.3389/fcimb.2016.00058. PubMed PMID: WOS:000377007400001.
 17. Thomas S, Holland IB, Schmitt L. The Type 1 secretion pathway - The hemolysin system and beyond. *Biochimica et biophysica acta*. 2013. doi: 10.1016/j.bbamcr.2013.09.017. PubMed PMID: 24129268.
 18. Delepelaire P. Type I secretion in gram-negative bacteria. *Biochimica et biophysica acta*. 2004;1694(1-3):149-61. doi: 10.1016/j.bbamcr.2004.05.001. PubMed PMID: 15546664.
 19. Binet R, Letoffe S, Ghigo JM, Delepelaire P, Wandersman C. Protein secretion by gram-negative bacterial ABC exporters. *Folia microbiologica*. 1997;42(3):179-83. PubMed PMID: 9246759.
 20. Wakeel A, den Dulk-Ras A, Hooykaas PJ, McBride JW. *Ehrlichia chaffeensis* tandem repeat proteins and Ank200 are type 1 secretion system substrates related to the repeats-in-toxin exoprotein family. *Frontiers in cellular and infection microbiology*. 2011;1:22. doi: 10.3389/fcimb.2011.00022. PubMed PMID: 22919588; PubMed Central PMCID: PMC3417381.
 21. Zhu B, Kuriakose JA, Luo T, Ballesteros E, Gupta S, Fofanov Y, et al. *Ehrlichia chaffeensis* TRP120 binds a G+C-rich motif in host cell DNA and exhibits eukaryotic transcriptional activator function. *Infection and immunity*. 2011;79(11):4370-81. doi: 10.1128/IAI.05422-11. PubMed PMID: 21859854; PubMed Central PMCID: PMC3257946.
 22. Luo T, Kuriakose JA, Zhu B, Wakeel A, McBride JW. *Ehrlichia chaffeensis* TRP120 interacts with a diverse array of eukaryotic proteins involved in transcription, signaling, and cytoskeleton organization. *Infection and immunity*.

- 2011;79(11):4382-91. doi: 10.1128/IAI.05608-11. PubMed PMID: 21859857; PubMed Central PMCID: PMC3257936.
23. Lin M, Rikihisa Y. Obligatory intracellular parasitism by *Ehrlichia chaffeensis* and *Anaplasma phagocytophilum* involves caveolae and glycosylphosphatidylinositol-anchored proteins. *Cellular microbiology*. 2003;5(11):809-20. PubMed PMID: 14531896.
 24. Luo T, Dunphy PS, Lina TT, McBride JW. *Ehrlichia chaffeensis* Exploits Canonical and Noncanonical Host Wnt Signaling Pathways to Stimulate Phagocytosis and Promote Intracellular Survival. *Infection and immunity*. 2015. doi: 10.1128/IAI.01289-15. PubMed PMID: 26712203.
 25. Lin M, Zhu MX, Rikihisa Y. Rapid Activation of Protein Tyrosine Kinase and Phospholipase C- γ 2 and Increase in Cytosolic Free Calcium Are Required by *Ehrlichia chaffeensis* for Internalization and Growth in THP-1 Cells. *Infection and immunity*. 2002;70(2):889-98. doi: 10.1128/iai.70.2.889-898.2002.
 26. Lina TT, Dunphy PS, Luo T, McBride JW. *Ehrlichia chaffeensis* TRP120 activates canonical notch signaling to downregulate TLR2/4 expression and promote intracellular survival. *MBio*. 2016;7(4):1–15.
 27. Zhu B, Farris TR, Milligan SL, Chen H, Zhu R, Hong A, et al. Rapid identification of ubiquitination and SUMOylation target sites by microfluidic peptide array. *Biochem Biophys Reports*. 2016;5:430–8.
 28. Dunphy PS, Luo T, McBride JW. *Ehrlichia chaffeensis* exploits Host SUMOylation pathways to mediate effector-host interactions and promote intracellular survival. *Infect Immun*. 2014;82(10):4154–68.
 29. Zhu B, Das S, Mitra S, Farris TR, McBride JW. *Ehrlichia chaffeensis* TRP120 moonlights as a HECT E3 ligase involved in self and host ubiquitination to influence protein interactions and stability for intracellular survival. *Infect Immun*. 2017;85(9).
 30. Wolf E, Eilers M, Popov N, Wolf E, Zhu J, Xu W, et al. Dual Regulation of Fbw7 Function and Oncogenic Transformation by Usp28. *Cell Reports*. 2014;9:1099–109.
 31. Schüle C, Eilers M, Popov N. PI3K-dependent phosphorylation of Fbw7 modulates substrate degradation and activity. *FEBS Lett*. 2011.
 32. Welcker M, Clurman BE. FBW7 ubiquitin ligase: a tumour suppressor at the crossroads of cell division, growth and differentiation. *Nat Rev Cancer* [Internet]. 2008;8(2):83–93. Available from: <http://www.nature.com/doi/10.1038/nrc2290>.
 33. Luo T, Dunphy PS, McBride JW. *Ehrlichia chaffeensis* Tandem Repeat Effector Targets Differentially Influence Infection. *Front Cell Infect Microbiol* [Internet]. 2017;7(May):1–16. Available from: <http://journal.frontiersin.org/article/10.3389/fcimb.2017.00178/full>.
 34. Paddock CD, Childs JE, Childs JE. *Ehrlichia chaffeensis*: a prototypical emerging pathogen. *Clin Microbiol Rev*. 2003;16(1):37–64.
 35. Rikihisa Y. Molecular events involved in cellular invasion by *Ehrlichia chaffeensis* and *Anaplasma phagocytophilum*. *Vet Parasitol*. 2010;167:155–66.

36. Mitra S, Dunphy PS, Das S, Zhu B, Luo T. *Ehrlichia chaffeensis* TRP120 Effector Targets and Recruits Host Polycomb Group Proteins for Degradation To Promote Intracellular Infection. *Infect Immun*. 2018;86(4):1–15.
37. Wakeel A, Zhu B, Yu X jie, McBride JW. New insights into molecular *Ehrlichia chaffeensis*-host interactions. *Microbes Infect* [Internet]. 2010;12(5):337–45. Available from: <http://dx.doi.org/10.1016/j.micinf.2010.01.009>.
38. Davis RJ, Welcker M, Clurman BE. Tumor suppression by the Fbw7Ubiquitin ligase: Mechanisms and opportunities. *Cancer Cell* [Internet]. 2014;26(4):455–64. Available from: <http://dx.doi.org/10.1016/j.ccell.2014.09.013>.
39. Takeishi S, Nakayama KI. Role of Fbxw7 in the maintenance of normal stem cells and cancer-initiating cells. *Br J Cancer*. 2014;111:1054–9.
40. Bray SJ. Notch signalling in context. *Nat Rev Mol Cell Biol* [Internet]. 2016;17(11):722–35. Available from: <http://dx.doi.org/10.1038/nrm.2016.94>.
41. Hori K, Sen A, Artavanis-Tsakonas S. Notch signaling at a glance. *J Cell Sci* [Internet]. 2013;126(10):2135–40. Available from: <http://jcs.biologists.org/cgi/doi/10.1242/jcs.127308>.
42. Shang Y, Smith S, Hu X. Role of Notch signaling in regulating innate immunity and inflammation in health and disease. *Protein Cell*. 2016;7(3):159–74.
43. Tanigaki K, Honjo T. Regulation of lymphocyte development by Notch signaling. *Nat Immunol*. 2007;8(5):451–6.
44. Eagar TN, Tang Q, Wolfe M, He Y, Pear WS, Bluestone JA. Notch 1 Signaling Regulates Peripheral T Cell Activation that Notch plays a critical role in the formation of many tissues, organs, and complex structures. *Immunity*. 2004;20:407–15.
45. Ostroukhova M, Qi Z, Oriss TB, Dixon-McCarthy B, Ray P, Ray A. Treg-mediated immunosuppression involves activation of the Notch-HES1 axis by membrane-bound TGF- β . *J Clin Invest*. 2006;116(4):996–1004.
46. Amsen D, Antov A, Jankovic D, Sher A, Radtke F, Souabni A, et al. Direct Regulation of Gata3 Expression Determines the T Helper Differentiation Potential of Notch. *Immunity*. 2007;27(1):89–99.
47. Narayana Y, Balaji KN. NOTCH1 up-regulation and signaling involved in *Mycobacterium bovis* BCG-induced SOCS3 expression in macrophages. *J Biol Chem*. 2008;283(18):12501–11.
48. Ito T, Allen RM, Carson IV WF, Schaller M, Cavassani KA, Hogaboam CM, et al. The critical role of Notch ligand delta-like 1 in the pathogenesis of influenza a virus (H1N1) infection. *PLoS Pathog*. 2011;7(11).
49. Min SH, Lau AW, Lee TH, Inuzuka H, Wei S, Huang P, et al. Negative Regulation of the Stability and Tumor Suppressor Function of Fbw7 by the Pin1 Prolyl Isomerase. *Mol Cell*. 2012;46:771–83.
50. Wang L, Ye X, Liu Y, Wei W, Wang Z. Aberrant regulation of FBW7 in cancer. *Oncotarget* [Internet]. 2014;5(8). Available from: <http://www.oncotarget.com/fulltext/1859>.

51. Yokobori T, Mimori K, Iwatsuki M, Ishii H, Onoyama I, Fukagawa T, et al. P53-altered FBXW7 expression determines poor prognosis in gastric cancer cases. *Cancer Res.* 2009;69(9):3788–94.
52. Ekholm-Reed S, Goldberg MS, Schlossmacher MG, Reed SI. Parkin-Dependent Degradation of the F-Box Protein Fbw7 Promotes Neuronal Survival in Response to Oxidative Stress by Stabilizing Mcl-1. *Mol Cell Biol* [Internet]. 2013;33(18):3627–43. Available from: <http://mcb.asm.org/cgi/doi/10.1128/MCB.00535-13>.
53. Kumadaki S, Karasawa T, Matsuzaka T, Ema M, Nakagawa Y, Nakakuki M, et al. Inhibition of ubiquitin ligase F-box and WD repeat domain-containing 7 α (Fbw7 α) causes hepatosteatosis through Krüppel-like Factor 5 (KLF5)/Peroxisome Proliferator-activated Receptor γ 2 (PPAR γ 2) pathway but not SREBP-1c protein in mice. *J Biol Chem.* 2011;286(47):40835–46.
54. Sancho R, Blake SM, Tendeng C, Clurman BE, Lewis J, Behrens A. Fbw7 Repression by Hes5 Creates a Feedback Loop That Modulates Notch-Mediated Intestinal and Neural Stem Cell Fate Decisions. *PLoS Biol.* 2013;11(6).
55. Jiang X, Xing H, Kim TM, Jung Y, Huang W, Yang HW, et al. Numb regulates glioma stem cell fate and growth by altering epidermal growth factor receptor and Skp1-Cullin-F-box ubiquitin ligase activity. *Stem Cells.* 2012;30(7):1313–26.
56. Minella AC, Clurman BE. Mechanisms of tumor suppression by the SCFFbw7. *Cell Cycle.* 2005;4(10):1356–9.
57. Inuzuka H, Shaik S, Onoyama I, Gao D, Tseng A, Maser RS, et al. SCFFBW7 regulates cellular apoptosis by targeting MCL1 for ubiquitylation and destruction. *Nature* [Internet]. 2011;471(7336):104–9. Available from: <http://www.nature.com/doi/10.1038/nature09732>.
58. Hoffman B, Liebermann DA. Apoptotic signaling by c-MYC. *Oncogene* [Internet]. 2008;27(50):6462–72. Available from: <http://www.nature.com/doi/10.1038/onc.2008.312>.
59. Fuchs SY. Tumor suppressor activities of the Fbw7 E3 ubiquitin ligase receptor. *Cancer Biol Ther.* 2005;4(5):506–8.
60. Welcker M, Larimore EA, Swanger J, Bengoechea-Alonso MT, Grim JE, Ericsson J, et al. Fbw7 dimerization determines the specificity and robustness of substrate degradation. *Genes Dev.* 2013.
61. Xu W, Taranets L, Popov N. Regulating Fbw7 on the road to cancer. *Semin Cancer Biol* [Internet]. 2015;1–9. Available from: <http://dx.doi.org/10.1016/j.semcancer.2015.09.005>.
62. Portnoy DA, Chen C, Mitchell G. Strategies Used by Bacteria to Grow in Macrophages. *Microbiol Spectr.* 2016;4(3).
63. Ernst RK, Guina T, Miller SI. How Intracellular Bacteria Survive: Surface Modifications That Promote Resistance to Host Innate Immune Responses. *J Infect Dis.* 2008;179(s2):S326–30.
64. Mehrlitz A, Rudel T. Modulation of host signaling and cellular responses by *Chlamydia*. *Cell Commun Signal.* 2013;11(1):1–11.

65. Ismail N, McBride JW. Tick-Borne Emerging Infections: Ehrlichiosis and Anaplasmosis. *Clin Lab Med* [Internet]. 2017;37(2):317–40. Available from: <http://dx.doi.org/10.1016/j.cll.2017.01.006>.
66. Carrieri FA, Dale JK. Turn It Down a Notch. *Front Cell Dev Biol* [Internet]. 2017;4(January):1–9. Available from: <http://journal.frontiersin.org/article/10.3389/fcell.2016.00151/full>.
67. Swafford D, Manicassamy S. Wnt Signaling in Dendritic Cells: Its Role in Regulation of Immunity and Tolerance. *Discov Med*. 2015;19(105):303–10.
68. Hu X, Chung AY, Wu I, Foldi J, Chen J, Ji JD, et al. Integrated Regulation of Toll-like Receptor Responses by Notch and Interferon- γ Pathways. *Immunity* [Internet]. 2008;29(5):691–703. Available from: <http://dx.doi.org/10.1016/j.immuni.2008.08.016>.
69. Zhang Q, Wang C, Liu Z, Liu X, Han C, Cao X, et al. Notch signal suppresses toll-like receptor-triggered inflammatory responses in macrophages by inhibiting extracellular signal-regulated kinase 1/2-mediated nuclear factor κ B activation. *J Biol Chem*. 2012;287(9):6208–17.
70. Balamurugan K, Wang JM, Tsai HH, Sharan S, Anver M, Leighty R, et al. The tumour suppressor C/EBP θ inhibits FBXW7 expression and promotes mammary tumour metastasis. *EMBO J* [Internet]. 2010;29(24):4106–17. Available from: <http://dx.doi.org/10.1038/emboj.2010.280>.
71. Balamurugan K, Sharan S, Klarmann KD, Zhang Y, Coppola V, Summers GH, et al. FBXW7 α attenuates inflammatory signalling by downregulating C/EBP δ and its target gene Tlr4. *Nat Commun* [Internet]. 2013;4:1612–62. Available from: <http://dx.doi.org/10.1038/ncomms2677>.
72. Rocher-Ros V, Marco S, Mao JH, Gines S, Metzger D, Chambon P, et al. Presenilin modulates EGFR signaling and cell transformation by regulating the ubiquitin ligase Fbw7. *Oncogene*. 2010;29(20):2950–61.
73. Kurashige J, Watanabe M, Iwatsuki M, Kinoshita K, Saito S, Hiyoshi Y, et al. Overexpression of microRNA-223 regulates the ubiquitin ligase FBXW7 in oesophageal squamous cell carcinoma. *Br J Cancer* [Internet]. 2012;106(1):182–8. Available from: <http://dx.doi.org/10.1038/bjc.2011.509>.
74. Wang Z, Fukushima H, Gao D, Inuzuka H, Wan L, Lau AW, et al. The two faces of FBW7 in cancer drug resistance. *BioEssays*. 2011;33(11):851–9.
75. Lerner M, Lundgren J, Akhoondi S, Jahn A, Ng HF, Moqadam FA, et al. MiRNA-27a controls FBW7/hCDC4-dependent cyclin E degradation and cell cycle progression. *Cell Cycle*. 2011;10(13):2172–83.
76. Enright AJ, Campos LS, Liu P, Dunham I, Siede J, Vigorito E, et al. MiR-25 Regulates Wwp2 and Fbxw7 and Promotes Reprogramming of Mouse Fibroblast Cells to iPSCs. *PLoS One*. 2012;7(8):e40938.
77. Palaga T, Buranaruk C, Rengpipat S, Fauq AH, Golde TE, Kaufmann SHE, et al. Notch signaling is activated by TLR stimulation and regulates macrophage functions. *Eur J Immunol*. 2008;38(1):174–83.

78. Davis RJ. Signal transduction by the JNK group of MAP kinases. *Cell*. 2000;103(2):239–52.
79. Vleugel MM, Greijer AE, Bos R, van der Wall E, van Diest PJ. c-Jun activation is associated with proliferation and angiogenesis in invasive breast cancer. *Hum Pathol*. 2006;37(6):668–74.
80. Farris TR, Dunphy PS, Zhu B, Kibler CE, McBride JW. *Ehrlichia chaffeensis* TRP32 is a nucleomodulin that directly regulates expression of host genes governing differentiation and proliferation. *Infect Immun*. 2016;84(11):3182–94.
81. Fujise K, Zhang D, Liu JL, Yeh ETH. Regulation of apoptosis and cell cycle progression by MCL1; Differential role of proliferating cell nuclear antigen. *J Biol Chem*. 2000;275(50):39458–65.
82. Bathina M, Lynch J, Perciavalle RM, Pelletier S, Opferman JT, Stewart DP, et al. Anti-apoptotic MCL-1 localizes to the mitochondrial matrix and couples mitochondrial fusion to respiration. *Nat Cell Biol* [Internet]. 2012;14(6):575–83. Available from: <http://dx.doi.org/10.1038/ncb2488>.
83. Penn LJ, Brooks MW, Laufer EM, Land H. Negative autoregulation of c-myc transcription. *EMBO J*. 1990;9(4):1113–21.
84. Nishide A, Kim M, Takagi K, Himeno A, Sanada T, Sasakawa C, et al. Structural basis for the recognition of Ubc13 by the *Shigella flexneri* effector ospi. *J Mol Biol* [Internet]. 2013;425(15):2623–31. Available from: <http://dx.doi.org/10.1016/j.jmb.2013.02.037>.
85. Kim DW, Lenzen G, Page A-L, Legrain P, Sansonetti PJ, Parsot C. The *Shigella flexneri* effector OspG interferes with innate immune responses by targeting ubiquitin-conjugating enzymes. *Proc Natl Acad Sci* [Internet]. 2005;102(39):14046–51. Available from: <http://www.pnas.org/cgi/doi/10.1073/pnas.0504466102>.
86. Sanada T, Kim M, Mimuro H, Suzuki M, Ogawa M, Oyama A, et al. The *Shigella flexneri* effector OspI deamidates UBC13 to dampen the inflammatory response. *Nature* [Internet]. 2012;483(7391):623–6. Available from: <http://dx.doi.org/10.1038/nature10894>.
87. Knodler LA, Winfree S, Drecktrah D, Ireland R, Steele-Mortimer O. Ubiquitination of the bacterial inositol phosphatase, SopB, regulates its biological activity at the plasma membrane. *Cell Microbiol*. 2009;11(11):1652–70.
88. Zhang Y, Higashide W, Dai S, Sherman DM, Zhou D. Recognition and ubiquitination of *Salmonella* type III effector SopA by a ubiquitin E3 ligase, HsRMA1. *J Biol Chem*. 2005;280(46):38682–8.
89. Kamanova J, Sun H, Lara-Tejero M, Galán JE. The *Salmonella* Effector Protein SopA Modulates Innate Immune Responses by Targeting TRIM E3 Ligase Family Members. *PLoS Pathog*. 2016;12(4):1–21.
90. Swatek KN, Komander D. Ubiquitin modifications. *Cell Res*. 2016;26(4):399–422.
91. Dumler JS, Madigan JE, Pusterla N, Bakkan JS. Ehrlichiosis in Humans: Epidemiology, Clinical Presentation, Diagnosis, and Treatment. *Clinical Infectious Diseases*, 2007;45: S45-S51.

92. Lin M, Rikihisa Y. *Ehrlichia chaffeensis* and *Anaplasma phagocytophilum* lack genes for lipid A biosynthesis and incorporate cholesterol for their survival. *Infect. Immun.* 2003;71(9): 5324-31.
93. Dunning Hotopp JC, Lin M, Madupu RF *et al.* Comparative genomics of emerging human ehrlichiosis agents. *PLoS Genet.* 2006;2:e21.
94. Pancholi V., Fischetti V. A. A major surface protein on group A streptococci is a glyceraldehyde-3-phosphate-dehydrogenase with multiple binding activity. *J. Exp. Med.* 1992. 176:415–426.
95. Lottenberg R., *et al.* Cloning, sequence analysis, and expression in *Escherichia coli* of a streptococcal plasmin receptor. *J. Bacteriol.* 1992. 174:5204–5210.
96. Winram S. B., Lottenberg R. The plasmin-binding protein Plr of group A streptococci is identified as glyceraldehyde-3-phosphate dehydrogenase. *Microbiology.* 1996. 142:2311–2320.
97. Pancholi V., Fischetti V. A. Glyceraldehyde-3-phosphate dehydrogenase on the surface of group A streptococci is also an ADP-ribosylating enzyme. *Proc. Natl. Acad. Sci.* 1993. 90:8154–8158.
98. Bergmann S., Rohde M., Hammerschmidt S. Glyceraldehyde-3-phosphate dehydrogenase of *Streptococcus pneumoniae* is a surface-displayed plasminogen-binding protein. *Infect. Immun.* 2004. 72:2416–2419.
99. Attali C., Durmort C., Vernet T., Di Guilmi A. M. The interaction of *Streptococcus pneumoniae* with plasmin mediates transmigration across endothelial and epithelial monolayers by intercellular junction cleavage. *Infect. Immun.* 2008. 76:5350–5356.
100. Pancholi V., Fischetti V. A. α -Enolase, a novel strong plasmin(ogen) binding protein on the surface of pathogenic streptococci. *J. Biol. Chem.* 1998. 273:14503–14515.
101. Candela M., *et al.* DnaK from *Bifidobacterium animalis* subsp. *lactis* is a surface-exposed human plasminogen receptor upregulated in response to bile salts. *Microbiology.* 2010. 156:1609–1618.
102. Santiago N. I., Zipf A., Bhunia A. K. Influence of temperature and growth phase on expression of a 104-kilodalton *Listeria* adhesion protein in *Listeria monocytogenes*. *Appl. Environ. Microbiol.* 1999. 65:2765–2769.
103. Wampler J. L., Kim K. P., Jaradat Z., Bhunia A. K. Heat shock protein 60 acts as a receptor for the *Listeria* adhesion protein in Caco-2 cells. *Infect. Immun.* 2004. 72:931–936.
104. Lin C. S., *et al.* A potential role for *Helicobacter pylori* heat shock protein 60 in gastric tumorigenesis. *Biochem. Biophys. Res. Commun.* 2010. 392:183–189.
105. Kamiya S., Yamaguchi H., Osaki T., Taguchi H. A virulence factor of *Helicobacter pylori*: role of heat shock protein in mucosal inflammation after *H. pylori* infection. *J. Clin. Gastroenterol.* 1998. 27:S35–39.
106. Kol A., Sukhova G. K., Lichtman A. H., Libby P. Chlamydial heat shock protein 60 localizes in human atheroma and regulates macrophage tumor necrosis factor- α and matrix metalloproteinase expression. *Circulation.* 1998. 98:300–307.

107. Costa C. P., et al. Role of chlamydial heat shock protein 60 in the stimulation of innate immune cells by *Chlamydia pneumoniae*. *Eur. J. Immunol.* 2002. 32:2460–2470.
108. Ausiello C. M., et al. 60-kDa heat shock protein of *Chlamydia pneumoniae* promotes a T helper type 1 immune response through IL-12/IL-23 production in monocyte-derived dendritic cells. *Microbes Infect.* 2006. 8:714–720.
109. Kalayoglu M. V., et al. Chlamydial virulence determinants in atherogenesis: the role of chlamydial lipopolysaccharide and heat shock protein 60 in macrophage-lipoprotein interactions. *J. Infect. Dis.* 2000. 181:S483–489.
110. Sasu S., LaVerda D., Qureshi N., Golenbock D. T., Beasley D. *Chlamydia pneumoniae* and chlamydial heat shock protein 60 stimulate proliferation of human vascular smooth muscle cells via Toll-like receptor 4 and p44/p42 mitogen-activated protein kinase activation. *Circ Res.* 2001. 89:244–250.
111. Van Montagu, M.; Holsters, M.; Zambryski, P.; Hernalsteens, J.P.; Depicker, A.; De Beuckeleer, M.; Engler, G.; Lemmers, M.; Willmitzer, L.; Schell, J. The interaction of *Agrobacterium* Ti-plasmid DNA and plant cells. *Proc. R. Soc. Lond. B Biol. Sci.* 1980, 210, 351–365.
112. Lebreton, A.; Lakisic, G.; Job, V.; Fritsch, L.; Tham, T.N.; Camejo, A.; Mattei, P.-J.; Regnault, B.; Nahori, M.-A.; Cabanes, D.; et al. A Bacterial Protein Targets the BAH1D1 Chromatin Complex to Stimulate Type III Interferon Response. *Science*, 2011, 331, 1319–1321.
113. Yang, N.; Xu, R.M. Structure and function of the BAH domain in chromatin biology. *Crit. Rev. Biochem. Mol. Biol.* 2013, 48, 211–221.
114. Prokop, A.; Gouin, E.; Villiers, V.; Nahori, M.A.; Vincentelli, R.; Duval, M.; Cossart, P.; Dussurget, O. OrfX, a Nucleomodulin Required for *Listeria monocytogenes* Virulence. *mBio* 2017, 8.
115. Zhan, S.; Wang, T.; Ge, W.; Li, J. Multiple roles of Ring 1 and YY1 binding protein in physiology and disease. *J. Cell Mol. Med.* 2018, 22, 2046–2054.
116. Chen, D.; Zhang, J.; Li, M.; Rayburn, E.R.; Wang, H.; Zhang, R. RYBP stabilizes p53 by modulating MDM2. *EMBO Rep.* 2009, 10, 166–172.
117. Dillon, S.C.; Zhang, X.; Trievel, R.C.; Cheng, X. The SET-domain protein superfamily: Protein lysine methyltransferases. *Genome Biol.* 2005, 6, 227.
118. Murata, M.; Azuma, Y.; Miura, K.; Rahman, M.A.; Matsutani, M.; Aoyama, M.; Suzuki, H.; Sugi, K.; Shirai, M. Chlamydial SET domain protein functions as a histone methyltransferase. *Microbiology.* 2007, 153, 585–592.
119. Pennini, M.S.P.; Dautry-Varsat, A.; Subtil, A. Histone methylation by NUP, a novel nuclear effector of the intracellular pathogen *Chlamydia trachomatis*. *PLoS Pathog.* 2010, 6, e1000995.
120. Rolando, M.; Sanulli, S.; Rusniok, C.; Gomez-Valero, L.; Bertholet, C.; Sahr, T.; Margueron, R.; Buchrieser, C. *Legionella pneumophila* effector RomA uniquely modifies host chromatin to repress gene expression and promote intracellular bacterial replication. *Cell Host Microbe.* 2013, 13, 395–405.

121. Li, T.; Lu, Q.; Wang, G.; Xu, H.; Huang, H.; Cai, T.; Kan, B.; Ge, J.; Shao, F. SET-domain bacterial effectors target heterochromatin protein 1 to activate host rDNA transcription. *EMBO Rep.* 2013, 14, 733–740.
122. Yaseen, I.; Kaur, P.; Nandicoori, V.K.; Khosla, S. *Mycobacteria* modulate host epigenetic machinery by Rv1988 methylation of a non-tail arginine of histone H3. *Nat. Commun.* 2015, 6, 8922.
123. Li, H.; Xu, H.; Zhou, Y.; Zhang, J.; Long, C.; Li, S.; Chen, S.; Zhou, J.-M.; Shao, F. The phosphothreonine lyase activity of a bacterial type III effector family. *Science.* 2007, 315, 1000–1003.
124. Singer, A.U.; Rohde, J.R.; Lam, R.; Skarina, T.; Kagan, O.; Dileo, R.; Chirgadze, N.Y.; Cuff, M.E.; Joachimiak, A.; Tyers, M.; et al. Structure of the *Shigella* T3SS effector IpaH defines a new class of E3 ubiquitin ligases. *Nat. Struct. Mol. Biol.* 2008, 15, 1293–1301.
125. Ashida, H.; Sasakawa, C. *Shigella* IpaH Family Effectors as a Versatile Model for Studying Pathogenic Bacteria. *Front. Cell Infect. Microbiol.* 2015, 5, 100.
126. Rohde, J.R.; Breitkreutz, A.; Chenal, A.; Sansonetti, P.J.; Parsot, C. Type III secretion effectors of the IpaH family are E3 ubiquitin ligases. *Cell Host Microbe.* 2007, 1, 77–83.
127. Toyotome, T. *Shigella* Protein IpaH9.8 Is Secreted from Bacteria within Mammalian Cells and Transported to the Nucleus. *J. Biol. Chem.* 2001, 276, 32071–32079.
128. Norkowski, S.; Schmidt, M.A.; Ruter, C. The species-spanning family of LPX-motif harbouring effector proteins. *Cell Microbiol.* 2018, 20, e12945.
129. Hicks, S.W.; Galan, J.E. Hijacking the host ubiquitin pathway: Structural strategies of bacterial E3 ubiquitin ligases. *Curr. Opin. Microbiol.* 2010, 13, 41–46.
130. Haraga, A.; Miller, S.I. A *Salmonella* type III secretion effector interacts with the mammalian serine/threonine protein kinase PKN1. *Cell Microbiol.* 2006, 8, 837–846.
131. Wei, C.; Wang, Y.; Du, Z.; Guan, K.; Cao, Y.; Yang, H.; Zhou, P.; Wu, F.; Chen, J.; Wang, P.; et al. The *Yersinia* Type III secretion effector YopM Is an E3 ubiquitin ligase that induced necrotic cell death by targeting NLRP3. *Cell Death Dis.* 2016, 7, e2519.
132. McDonald, C.; Vacratsis, P.O.; Bliska, J.B.; Dixon, J.E. The *Yersinia* virulence factor YopM forms a novel protein complex with two cellular kinases. *J. Biol. Chem.* 2003, 278, 18514–18523.
133. McCoy, M.W.; Marre, M.L.; Lesser, C.F.; Meccas, J. The C-terminal tail of *Yersinia pseudotuberculosis* YopM is critical for interacting with RSK1 and for virulence. *Infect. Immun.* 2010, 78, 2584–2598.
134. Valleau, D.; Little, D.J.; Borek, D.; Skarina, T.; Quaile, A.T.; Di Leo, R.; Houlston, S.; Lemak, A.; Arrowsmith, C.H.; Coombes, B.K.; et al. Functional diversification of the NleG effector family in enterohemorrhagic *Escherichia coli*. *Proc. Natl. Acad. Sci. USA.* 2018, 115, 10004–10009.

135. Werden, S.J.; Lanchbury, J.; Shattuck, D.; Neff, C.; Dufford, M.; McFadden, G. The myxoma virus m-t5 ankyrin repeat host range protein is a novel adaptor that coordinately links the cellular signaling pathways mediated by Akt and Skp1 in virus-infected cells. *J. Virol.* 2009, 83, 12068–12083.
136. Min, C.K.; Kwon, Y.J.; Ha, N.Y.; Cho, B.A.; Kim, J.M.; Kwon, E.K.; Kim, Y.S.; Choi, M.S.; Kim, I.S.; Cho, N.H. Multiple *Orientia tsutsugamushi* ankyrin repeat proteins interact with SCF1 ubiquitin ligase complex and eukaryotic elongation factor 1 alpha. *PLoS ONE*. 2014, 9, e105652.
137. Sun, H.; Kamanova, J.; Lara-Tejero, M.; Galan, J.E. A Family of *Salmonella* Type III Secretion Effector Proteins Selectively Targets the NF-kappaB Signaling Pathway to Preserve Host Homeostasis. *PLoS Pathog.* 2016, 12, e1005484.
138. Jennings, E.; Esposito, D.; Rittinger, K.; Thurston, T.L.M. Structure-function analyses of the bacterial zinc metalloprotease effector protein GtgA uncover key residues required for deactivating NF-kappaB. *J. Biol. Chem.* 2018, 293, 15316–15329.
139. Mosavi, L.K.; Cammett, T.J.; Desrosiers, D.C.; Peng, Z.Y. The ankyrin repeat as molecular architecture for protein recognition. *Protein Sci.* 2004, 13, 1435–1448.
140. Wakeel, A.; den Dulk-Ras, A.; Hooykaas, P.J.; McBride, J.W. *Ehrlichia chaffeensis* tandem repeat proteins and Ank200 are type 1 secretion system substrates related to the repeats-in-toxin exoprotein family. *Front. Cell Infect. Microbiol.* 2011, 1, 22.
141. Kibler, C.E.; Milligan, S.L.; Farris, T.R.; Zhu, B.; Mitra, S.; McBride, J.W. *Ehrlichia chaffeensis* TRP47 enters the nucleus via a MYND-binding domain-dependent mechanism and predominantly binds enhancers of host genes associated with signal transduction, cytoskeletal organization, and immune response. *PLoS ONE*. 2018, 13, e0205983.
142. Diao J, Zhang Y, Huibregtse JM, Zhou D, Chen J. Crystal structure of SopA, a *Salmonella* effector protein mimicking a eukaryotic ubiquitin ligase. *Nat Struct Mol Biol.* 2008. 15:65–70. doi:10.1038/nsmb1346.
143. Zhang Y, Higashide WM, McCormick BA, Chen J, Zhou D. The inflammation-associated *Salmonella* SopA is a HECT-like E3 ubiquitin ligase. *Mol Microbiol.* 2006. 62:786–793. doi:10.1111/j.1365-2958.2006.05407.
144. Hartwell, L. H., Mortimer, R. K., Culotti, J. & Culotti, M. Genetic control of the cell division cycle in yeast: V. genetic analysis of cdc mutants. *Genetics*. 1973. 74, 267–286.
145. Schwob, E., Bohm, T., Mendenhall, M. D. & Nasmyth, K. The B-type cyclin kinase inhibitor p40SIC1 controls the G1 to S transition in *S. cerevisiae*. *Cell*. 1994. 79, 233–244.
146. Perkins, G., Drury, L. S. & Diffley, J. F. Separate SCF^{CDC4} recognition elements target Cdc6 for proteolysis in S phase and mitosis. *EMBO J.* 2001. 20, 4836–4845.
147. Sundaram, M. & Greenwald, I. Suppressors of a lin-12 hypomorph define genes that interact with both lin-12 and glp-1 in *Caenorhabditis elegans*. *Genetics*. 1993. 135, 765–783.

148. Hubbard, E. J., Wu, G., Kitajewski, J. & Greenwald, I. Sel-10, a negative regulator of lin-12 activity in *Caenorhabditis elegans*, encodes a member of the CDC4 family of proteins. *Genes Dev.* 1997. 11, 3182–3193.
149. Moberg, K. H., Bell, D. W., Wahrer, D. C., Haber, D. A. & Hariharan, I. K. Archipelago regulates Cyclin E levels in *Drosophila* and is mutated in human cancer cell lines. *Nature.* 2001. 413, 311–316.
150. Spruck, C. H. et al. hCDC4 gene mutations in endometrial cancer. *Cancer Res.* 2002. 62, 4535–4539.
151. Matsumoto, A., Onoyama, I. & Nakayama, K. I. Expression of mouse *Fbxw7* isoforms is regulated in a cell cycle- or p53-dependent manner. *Biochem. Biophys. Res. Commun.* 2006. 350, 114–119.
152. Kimura, T., Gotoh, M., Nakamura, Y. & Arakawa, H. hCDC4b, a regulator of cyclin E, as a direct transcriptional target of p53. *Cancer Sci.* 2003. 94, 431–436.
153. Welcker, M., Orian, A., Grim, J. E., Eisenman, R. N. & Clurman, B. E. A nucleolar isoform of the Fbw7 ubiquitin ligase regulates c-Myc and cell size. *Curr. Biol.* 2004. 14, 1852–1857.
154. Bai, C. et al. SKP1 connects cell cycle regulators to the ubiquitin proteolysis machinery through a novel motif, the F-box. *Cell.* 1996. 86, 263–274.
155. Orlicky, S., Tang, X., Willems, A., Tyers, M. & Sicheri, F. Structural basis for phosphodependent substrate selection and orientation by the SCFCdc4 ubiquitin ligase. *Cell.* 2003. 112, 243–256.
156. Hao, B., Oehlmann, S., Sowa, M. E., Harper, J. W. & Pavletich, N. P. Structure of a Fbw7–Skp1–cyclin E complex: multisite-phosphorylated substrate recognition by SCF ubiquitin ligases. *Mol. Cell.* 2007. 26, 131–143.
157. Tang, X. et al. Suprafacial orientation of the SCFCdc4 dimer accommodates multiple geometries for substrate ubiquitination. *Cell.* 2007. 129, 1165–1176.
158. Welcker, M. & Clurman, B. E. Fbw7/hCDC4 dimerization regulates its substrate interactions. *Cell Div.* 2007. 2, 7.
159. Klinakis, A. et al. Myc is a Notch1 transcriptional target and a requisite for Notch1-induced mammary tumorigenesis in mice. *Proc. Natl Acad. Sci. USA.* 2006. 103, 9262–9267.
160. Weng, A. P. et al. c-Myc is an important direct target of Notch1 in T-cell acute lymphoblastic leukemia/lymphoma. *Genes Dev.* 2006. 20, 2096–2109.
161. Wu, G., Hubbard, E. J., Kitajewski, J. K. & Greenwald, I. Evidence for functional and physical association between *Caenorhabditis elegans* SEL-10, a Cdc4p-related protein, and SEL-12 presenilin. *Proc. Natl Acad. Sci. USA.* 1998. 95, 15787–15791.
162. Knuutila, S. et al. DNA copy number losses in human neoplasms. *Am. J. Pathol.* 1999. 155, 683–694.
163. Kimura T, Gotoh M, Nakamura Y and Arakawa H. hCDC4b, a regulator of cyclin E, as a direct transcriptional target of p53. *Cancer Sci.* 2003; 94(5):431-436.
164. Mao JH, Perez-Losada J, Wu D, Delrosario R, Tsunematsu R, Nakayama KI, Brown K, Bryson S and Balmain A. Fbxw7/Cdc4 is a p53-dependent, haploinsufficient tumour suppressor gene. *Nature.* 2004; 432(7018):775-779.

165. Feng DD, Zhang H, Zhang P, Zheng YS, Zhang XJ, Han BW, Luo XQ, Xu L, Zhou H, Qu LH and Chen YQ. Downregulated miR-331-5p and miR-27a are associated with chemotherapy resistance and relapse in leukemia. *J Cell Mol Med.* 2010.
166. Durgan, J., and Parker, P.J. Regulation of the tumour suppressor Fbw7a by PKC-dependent phosphorylation and cancer-associated mutations. *Biochem. J.* 2010. 432, 77–87.
167. Min, S.-H., Lau, A.W., Lee, T.H., Inuzuka, H., Wei, S., Huang, P., Shaik, S., Lee, D.Y., Finn, G., Balastik, M., et al. Negative regulation of the stability and tumor suppressor function of Fbw7 by the Pin1 prolyl isomerase. *Mol. Cell.* 2012. 46,771–783.
168. Mitchell G, Chen C, Portnoy DA. Strategies used by bacteria to grow in macrophages. *Microbiol Spectr.* 2016;4(3).
169. Yada M, Hatakeyama S, Kamura T, Nishiyama M, Tsunematsu R, Imaki H, et al. Phosphorylation-dependent degradation of c-Myc is mediated by the F-box protein Fbw7. *EMBO J.* 2004;23(10):2116–25.
170. Koepp DM, Schaefer LK, Ye X, Keyomarsi K, Chu C, Harper JW, et al. Phosphorylation-dependent ubiquitination of cyclin E by the SCFFbw7 ubiquitin ligase. *Science.* 2001;294(5540):173–7.
171. Öberg C, Li J, Pauley A, Wolf E, Gurney M, Lendahl U. The Notch intracellular domain is ubiquitinated and negatively regulated by the mammalian Sel-10 homolog. *J Biol Chem.* 2001;276(38):35847–53.
172. Durgan J, Parker PJ. Regulation of the tumour suppressor Fbw7 α by PKC-dependent phosphorylation and cancer-associated mutations. *Biochem J.* 2010;432(1):77–87.
173. Wang Y, Zhang P, Wang Y, Zhan P, Liu C, Mao JH, et al. Distinct interactions of EBP1 isoforms with FBXW7 elicits different functions in cancer. *Cancer Res.* 2017;77(8):1983–96.
174. Balamurugan K, Wang JM, Tsai HH, Sharan S, Anver M, Leighty R, et al. The tumour suppressor C/EBP θ inhibits FBXW7 expression and promotes mammary tumour metastasis. *EMBO J* [Internet]. Nature Publishing Group; 2010;29(24):4106–17.
175. Aguiar DM, Ziliani TF, Zhang X, Melo ALT, Braga IA, Witter R, et al. A novel *Ehrlichia* genotype strain distinguished by the TRP36 gene naturally infects cattle in Brazil and causes clinical manifestations associated with ehrlichiosis. *Ticks and Tick-borne Diseases.* 2014; 5(5): 537-544.
176. Buller RS, Arens M, Hmiel SP, Paddock CD, Sumner JW, Rikihisa Y, et al. *Ehrlichia ewingii*, a newly recognized agent of human ehrlichiosis. *N Engl J. Med.* 1999; 341:148-155.
177. Perez M, Bodor M, Zhang C, Xiong Q, Rikihisa Y. Human infection with *Ehrlichia canis* accompanied by clinical signs in Venezuela. *Ann. N.Y. Acad. Sci.* 2006; 1078: 110-7.

178. Biguezoton A, Noel V, Adehan S, et al. *Ehrlichia ruminantium* infects *Rhipicephalus microplus* in West Africa. *Parasites Vectors*. 2016; 9, 354. <https://doi.org/10.1186/s13071-016-1651-x>.
179. Biggs HM, Behravesh CB, Bradley KK, et al. Diagnosis and management of tickborne rickettsial diseases: Rocky Mountain Spotted Fever and other spotted fever group rickettsioses, ehrlichiosis, and anaplasmosis – United States. *Recommendations and Reports*. 2016; 65(2): 1-48.
180. Dumler JS, Bakken JS. Ehrlichial diseases of humans: emerging tick-borne infections. *Clin. Infect. Dis*. 1995; 20:1102-10.
181. Dumler JS, Walker DH. Tick-borne ehrlichiosis. *Lancet Infectious Diseases*. 2001; 1:21-28.
182. Dumler JS, Bakken JS. Human ehrlichiosis: newly recognized infections transmitted by ticks. *Annu Rev Med*. 1998; 49:201-13.
183. Olano JP, Walker DH. Human ehrlichiosis. *Med. Clin. North Am*. 2002; 86:375-92.
184. Liddell AM, Sumner JW, Paddock CD, Rikihisa Y, Unver A, Buller RS, Storch GA. Reinfection with *Ehrlichia chaffeensis* in a liver transplant recipient. *Clin Infect Dis*. 2002; 34:1644-47.
185. Paddock CD, Folk SM, Shore GM, Machado LJ, Huycke MM, et al. Infections with *Ehrlichia chaffeensis* and *Ehrlichia ewingii* in persons coinfecting with human immunodeficiency virus. *Clin Infect Dis*. 2001; 33:1586-94.
186. Talbot TR, Comer JA, Bloch KC. *Ehrlichia chaffeensis* infections among HIV-infected patients in a human monocytic ehrlichiosis-endemic area. *Emerg Infect Dis*. 2003; 9:1123-27.
187. Brouqui P, Raoult D. *In vitro* antibiotic susceptibility of the newly recognized agent of ehrlichiosis in humans, *Ehrlichia chaffeensis*. *Antimicrob Agents Chemother*. 1992; 36(12):2799-803.
188. Everett ED, Evans KA, Henry RB, McDonald G. Human ehrlichiosis in adults after tick exposure. Diagnosis using polymerase chain reaction. *Ann Intern Med*. 1994; 120:730-735.
189. Walker DH, Dumler JS. *Ehrlichia chaffeensis* human monocytopathic ehrlichiosis., *Ehrlichia phagocytophila* human granulocytotropic ehrlichiosis., and other Ehrlichiae. In: Mandell GL, Bennett JE, Dolin R, eds. *Principles and Practice of Infectious Diseases*. Fifth ed. Philadelphia, PA: Churchill Livingstone; 2000: 2057-64.
190. Eng TR, Harkess JR, Fishbein DB, Dawson JE, Greene CN, Redus MA, and Satalowich FT. Epidemiologic, clinical, and laboratory findings of human ehrlichiosis in the United States. *JAMA*. 1990; 264:2251-2258.
191. Ewing SA, Dawson JE, Kocan AA, Barker RW, Warner CK, Panciera RJ, Fox JC, Kocan KM, and Blouin EF. Experimental transmission of *Ehrlichia chaffeensis* (Rickettsiales: Ehrlichieae) among white-tailed deer by *Amblyomma americanum* (Acari: Ixodidae). *J. Med. Entomol*. 1995; 32:368-374.

192. Fishbein DB, Dawson JE, and Robinson LE. Human ehrlichiosis in the United States, 1985 to 1990. *Ann. Intern. Med.* 1994; 120:736-743.
193. Standaert SM, Dawson JE, Schaffner W, Childs JE, Biggie KL, Singleton Jr J, Gerhardt RR, Knight ML, and Hutcheson RH. Ehrlichiosis in a golf-oriented retirement community. *N. Engl. J. Med.* 1995; 333:420-425.
194. McQuiston JH, Paddock CD, Holman RC, and Childs JE. The human ehrlichioses in the United States. *Emerg. Infect. Dis.* 1999; 5:635-642.
195. IJdo JW, Wu C, Magnarelli LA, Stafford KC, Anderson JF, and Fikrig E. Detection of *Ehrlichia chaffeensis* DNA in *Amblyomma americanum* ticks in Connecticut and Rhode Island. *J. Clin. Microbiol.* 2000; 38:4655-4656.
196. Barnewall RE, Rikihisa Y, Lee EH. *Ehrlichia chaffeensis* inclusions are early endosomes which selectively accumulate transferrin receptor. *Infect Immun.* 1997; 65(4):1455-61.
197. Cheng Y, Liu Y, Wu B, Zhang JZ, Gu J, Liao YL, Wang FK, Mao XH, Yu XJ. Proteomic analysis of the *Ehrlichia chaffeensis* phagosome in cultured DH82 cells. *PLoS One.* 2014; 9(2):e88461.
198. Mavromatis K, Doyle CK, Lykidis A, Ivanova N, Francino MP, Chain P, Shin M, Malfatti S, Larimer F, Copeland A, Detter JC, Land M, Richardson PM, Yu XJ, Walker DH, McBride JW, Kyrpides NC. The genome of the obligately intracellular bacterium *Ehrlichia canis* reveals themes of complex membrane structure and immune evasion strategies. *J Bacteriol.* 2006; 188(11):4015-23.
199. Henderson B. An overview of protein moonlighting in bacterial infection. *Biochem Soc Trans.* 2014; 42(6): 1720-7.
200. Chang GC, Liu KJ, Hsieh CL, et al. Identification of α -enolase as an autoantigen in lung cancer: its overexpression is associated with clinical outcomes. *Clinical Cancer Research.* 2006; 12(19): 5746-54.
201. Lopez-Pedrerera C, Villalba JM, Siendones E, et al. Proteomic analysis of acute myeloid leukemia: identification of potential early biomarkers and therapeutic targets. *Proteomics.* 2006; 6:S293-9.
202. Kinloch A, Tatzer V, Wait R, et al. Identification of citrullinated alpha-enolase as a candidate autoantigen in rheumatoid arthritis. *Arthritis Research & Therapy.* 2005; 7(6): R1421-9.
203. Butterfield DA and Lange MLB. Multifunctional roles of enoase in Alzheimer's disease brain: beyond altered glucose metabolism. *Journal of Neurochem.* 2009; 111(4): 915-33.
204. Pancholi V. Multifunctional α -enolase: its role in diseases. *Cellular and Molecular Life Sciences.* 2001; 58(7): 902–20.
205. Hattori T, Takei N, Mizuno Y, Kato K, Kohsaka S. Neurotrophic and neuroprotective effects of neuron-specific enolase on cultured neurons from embryonic rat brain. *Neurosci Res.* 1995; 21(3):191-8.
206. Iida H, Yahara I. Yeast heat-shock protein of M_r 48,000 is an isoprotein of enolase. *Nature.* 1985; 315:688–690.

207. Aaronson RM, Graven KK, Tucci M, McDonald RJ, Farber HW. Non-neuronal enolase is an endothelial hypoxic stress protein. *J Biol Chem*. 1995; 270(46):27752-7.
208. Subramanian A, Miller DM. Structural analysis of alpha-enolase. Mapping the functional domains involved in down-regulation of the *c-myc* protooncogene. *J Biol Chem*. 2000; 275(8):5958-65.
209. Lina TT, LuoT, Velayutham TS, Das S, McBride JW. *Ehrlichia* activation of Wnt-PI3K-mTOR signaling inhibits autolysosome generation and autophagic destruction by the mononuclear phagocyte. *Infect Immun*. 2017; 85:e00690-17. Doi: 10.1128/IAI.00690-17.

Curriculum Vitae

Education:

University of Texas Medical Branch, Galveston, TX
Ph. D. – Cell Biology
2014 – 2020

University of Washington, Seattle, WA
B. S. – Microbiology
2007 – 2011

Professional Experience:

University of Texas Medical Branch, Galveston, TX
Graduate Research Assistant
September 2014 – May 2020

Fred Hutchinson Cancer Research Center, Seattle, WA
Research Technician I
October 2010 – July 2014

Additional Experience:

2019 **Business Development BootCamp** by Enventure
2018 **The Process of Drug Development eLearning Course** by Lilly
 Pharmaceuticals

Publications:

Wang JY, Zhu B, Patterson LL, Rogan MR, Kibler CE and McBride JW (2020). *Ehrlichia chaffeensis* TRP120-mediated ubiquitination and proteasomal degradation of tumor suppressor FBW7 increases oncoprotein stability and promotes infection. *PLOS Pathogens*. 16(4): e1008541. <https://doi.org/10.1371/journal.ppat.1008541>.

Rogan MR, Patterson LL, **Wang JY** and McBride JW (2019). Bacterial manipulation of Wnt signaling: A host-pathogen tug-of-Wnt. *Front. Immunol.* 10:2390. doi: 10.3389/fimmu.2019.0239.

Farris TR, Zhu B, **Wang JY** and McBride JW (2017). *Ehrlichia chaffeensis* TRP32 nucleomodulin function and localization is regulated by NEDD4L-mediated ubiquitination. *Front. Cell Infect. Microbiol.* 7:534. doi: 10.3389/fcimb.2017.00534.

Yu M, Trobridge P, **Wang Y**, Kannurn S, Morris SM, Knoblauch S and Grady WM (2014). Inactivation of Tgfb signaling and loss of PTEN cooperate to induce colon cancer *in vivo*. *Oncogenes*. 33(12): 1538-1547. doi: 10.1038/onc.2013.102.

Select Posters/Presentations:

Wang JY and McBride JW. Degradation of tumor suppressor FBW7 by *Ehrlichia chaffeensis* TRP120-mediated ubiquitination promotes infection. American Society for Rickettsiology Conference. June 2019. Santa Fe, NM.

Wang JY, Zhu B and McBride JW. *Ehrlichia chaffeensis* TRP120 HECT Ub ligase targets FBW7 for degradation to maintain Notch signaling to promote infection. American Society for Rickettsiology Conference. June 2018. Milwaukee, WI.

Wang JY, Luo T and McBride JW. *Ehrlichia chaffeensis* TRP120 enhances Notch signaling by targeting SCF ubiquitin ligase FBW7 for degradation. American Society for Microbiology Conference. June 2017. New Orleans, LA.

Wang JY, Luo T and McBride JW. *Ehrlichia chaffeensis* TRP120 influences Notch signaling and cell cycle by modulating the SCF ubiquitin ligase FBW7 to promote infection. American Society for Rickettsiology. June 2016. Big Sky, MT.

Scholarships and Awards:

2018-2020	McLaughlin Predoctoral Fellowship at UTMB
2019	Oral Presentation 2nd Place at 6 th Annual Student Symposium by CBGP (UTMB)
2018	The Edward S. Reynolds Award at Dept. of Pathology 24 th Annual Trainee Research Day (UTMB)
2018	James W. McLaughlin Travel Award at 2018 IHII/McLaughlin Colloquium (UTMB)
2017	Oral Presentation 2nd Place at 4 th Annual Student Symposium by CBGP (UTMB)
2017	The Edward S. Reynolds Award at Dept. of Pathology 23 rd Annual Trainee Research Day (UTMB)

Certification:

BSL-2 Certified

Permanent address: 13506 Wild Lilac Ct., Pearland, TX 77584

This dissertation was typed by Jennifer Y. Wang